Proportional-Integral Control in the Evaluation of Glucose Homeostasis and Type 2 Diabetes

Jaycee Kaufman

A thesis submitted to the School of Graduate and Postdoctoral Studies in partial fulfillment of the requirements for the degree of

Master of Science in Modelling and Computational Science

Faculty of Science

University of Ontario Institute of Technology (Ontario Tech University)

Oshawa, Ontario, Canada

March 2022

THESIS EXAMINATION INFORMATION

Submitted by: **Jaycee Kaufman**

Master of Science in Modelling and Computational Science

Thesis Title:
Proportional-Integral Control in the Evaluation of Glucose Homeostasis and Type 2 Diabetes

An oral defense of this thesis took place on April 29, 2022 in front of the following examining committee:

Examining Committee:

Chair of Examining Committee	Greg Lewis
Research Supervisor	Lennaert van Veen
Examining Committee Member	Jane Breen
Thesis Examiner	Hendrick de Haan

The above committee determined that the thesis is acceptable in form and content and that a satisfactory knowledge of the field covered by the thesis was demonstrated by the candidate during an oral examination. A signed copy of the Certificate of Approval is available from the School of Graduate and Postdoctoral Studies.

ABSTRACT

Glucose, a simple sugar, is a main source of energy for the majority of cells in our body. When the glucose concentration in the blood is ill-controlled and glucose levels become too high, the individual is said to have diabetes. Mathematical modelling of blood sugar dynamics has been explored since the early 1960s. However, for most of these models, to find parameter values that yield plausible glucose behaviour one needs measurements of regulatory hormones such as insulin and glucagon. These hormone measurements require repeated blood tests and limit the feasibility of applying the model to "real world" medical applications such as disease diagnosis. Here, we apply a proportional-integral control model to human glucose homeostasis. With this "closed-loop" approach, measurements of hormone concentrations do not need to be taken. The model can be fit and tuned using glucose time series data obtained exclusively from a continuous glucose monitor. The resulting parameters from model tuning can then be used as an evaluation of the effectiveness of an individual's blood glucose homeostasis. Furthermore, when we apply the model to glucose data from individuals with type 2 diabetes or prediabetes, these parameter values can be used as a biomarker to predict the diabetic status of an individual. This research has the potential to be a future diagnostic or intervention tool in type 2 diabetes and may aid in the early prediction of prediabetes.

Keywords: Glucose Homeostasis, Diabetes, Proportional-Integral Control, Math Modelling

AUTHOR'S DECLARATION

I hereby declare that this thesis consists of original work of which I have authored. This is a true copy of the thesis, including any required final revisions, as accepted by my examiners.

I authorize the University of Ontario Institute of Technology (Ontario Tech University) to lend this thesis to other institutions or individuals for the purpose of scholarly research. I further authorize University of Ontario Institute of Technology (Ontario Tech University) to reproduce this thesis by photocopying or by other means, in total or in part, at the request of other institutions or individuals for the purpose of scholarly research. I understand that my thesis will be made electronically available to the public.

The research work in this thesis that was performed in compliance with the regulations of Research Ethics Board under **NCT04077203, NCT04529239, & CTRI/2021/08/035957**.

_____ JAYCEE KAUFMAN

STATEMENT OF CONTRIBUTIONS

This thesis focuses on the application of a proportional-integral control dynamical system model to healthy individuals and individuals with type 2 diabetes. All work presented in this thesis is my own, with the following exceptions:

1. Model development and gradient descent implementation was done by Lennaert van Veen and Jacob Morra.
2. The automated peak selection was implemented by Kathryn Chen.
3. The global stability analysis presented in Chapter 3 was calculated by Eric Ng and Lennaert van Veen.

The work presented in Section 3.2 has been submitted for publication, and is currently in review.

ACKNOWLEDGEMENTS

This project would not have been possible without a number of people. First, I'd like to thank my committee members, Dr. Lennaert van Veen, Dr. Jane Breen, and Yan Fossat for the support and inspiration they have provided me throughout my Master's degree. This thesis would not be possible without the feedback and discussion you all have provided.

Next, I would like to recognize the invaluable contributions made by Eric Ng. Many of the results presented in this thesis would not have emerged without your help or our weekly discussions. I also gratefully acknowledge the work done by Jacob Morra and Kathryn Chen in the initial phases of the project, whose contributions laid the groundwork for this thesis and analysis.

I would also like to thank Klick Health and the employees who have provided support in this project - specifically Adam, Ani, and Jessie from the Labs team. Thank you for the many conversations about interesting science and technology and for welcoming me into your workplace.

Finally, I am forever grateful for my partner Dario and my parents, whose continuous love and support has allowed me to fully immerse myself in this research. I would not be the person I am today without them, and this thesis is dedicated to them.

TABLE OF CONTENTS

LIST OF TABLES

LIST OF FIGURES

LIST OF ABBREVIATIONS AND SYMBOLS

CGM: Continuous Glucose Monitor

SNS: Sympathetic Nervous System

T2D: Type 2 Diabetes

HbA1c: Hemoglobin A1c

OGTT: Oral Glucose Tolerance Test

FBG: Fasting Blood Glucose

σ: Standard Deviation

φ: Range

1 Introduction

1.1 Glucose Homeostasis and Diabetes

The term "*Homeostasis*" was coined by Walter Cannon in 1926, where it was defined as the mechanisms employed by biological organisms in order to maintain a steady state. Changes in the external environment result in adjustments to the internal environment, which are corrected by automated physiological processes [1]. In the human body, many homeostatic mechanisms are constantly functioning in order to keep all systems within a healthy range. The amount of water in the body is regulated by the kidneys and the temperature is regulated by blood flow, sweat, and shivering. Homeostasis in the human body allows the individual to experience changes in their external environment without experiencing change internally [2].

Arguably one of the most important examples of homeostasis is the regulation of glucose within the bloodstream. Glucose is a high energy molecule that is used as a primary energy source by the majority of cells in the body. It is obtained from breaking down and digesting foods such as carbohydrates, fruits, vegetables, and milk products. Glucose is absorbed from the gastrointestinal tract through the small intestine, where it then travels to the liver to be distributed throughout the body or stored as glycogen [3].

If glucose levels in the bloodstream are not within a specific range, the individual can experience negative side effects. If blood glucose levels are too low, the individual may experience anxiety, fatigue, weakness, nausea, dizziness or lightheadedness. If the individual's blood glucose remains low they may even experience coma or death [4]. Alternatively, if the individual's blood glucose is too high, they may be fatigued, nauseous, have shortness of breath, stomach pain or a rapid heartbeat. If periods of high blood glucose are extended for long periods of time, the individual could experience coma or death [5]. Ultimately, it is vital for the individual to keep the glucose levels within the optimal range .

To keep glucose levels constant, the body primarily employs hormonal control. If blood glucose levels are too high, the pancreas releases insulin to stimulate fat cells to convert and store glucose as fatty acids. If blood glucose levels are too low, the pancreas releases glucagon which stimulates the liver to break down the stored glycogen and release the glucose into the bloodstream, and eating foods rich in glucose can raise blood glucose levels. Furthermore, the sympathetic nervous system (SNS) can also increase blood glucose levels. The SNS is responsible for the "flight or fight" response. When an individual is exposed to stress, the SNS stimulates the relase of epinephrine, also known as adrenaline, in order to prepare the body to fight the source of stress or flee from it. Along with increasing the heart rate and blood pressure, and dilating the pupils and the airways of the lungs, Epinephrine also acts to increase blood glucose levels. [3].

When the body is unable to control high blood glucose levels through insulin action, the individual is diabetic. The type of diabetes an individual has is dependent on which part of the homeostatic mechanism is dysfunctional. If the individual is unable to produce sufficient insulin from pancreatic beta cells, they are Type 1 Diabetic. This type of diabetes is typically a result of genetics or autoimmune disease. These individuals can replicate pancreatic release of insulin by injecting themselves with the hormone. By constantly monitoring blood glucose levels and injecting insulin accordingly, individuals with Type 1 Diabetes recover some functionality of their glucose control system [6]. Alternatively, individuals who are able to produce insulin but are unable to respond to it have Type 2 Diabetes (T2D). This type of diabetes is typically caused by lifestyle - if individuals constantly have high blood glucose levels they are more likely to develop T2D. Injecting insulin does not have as much of an effect for individuals with T2D. Overall, individuals with untreated diabetes (both Type 1 and Type 2) have sustained periods of high blood glucose [6].

The CDC estimates that over 34 million Americans have diabetes, corresponding to approximately 1 in 10 individuals. Of these individuals, 90-95% of diabetic individuals are Type 2 Diabetic [7]. This is costing the American healthcare system over $237 billion in direct medical costs [8]. It is thus of

medical interest to identify as many individuals as possible who may progress to T2D in an effort to start preventative measures early.

The stage before an individual becomes Type 2 Diabetic is called Prediabetic. This stage is much easier to reverse than if an individual is fully Type 2 Diabetic. Diet, exercise, and weight loss have been shown to drastically reduce the risk of prediabetes progressing to type 2 diabetes, with the CDC estimating that the risk of progressing can be reduced up to 58% [9]. The more individuals who are identified to be in this stage and given a regimen of diet and exercise, the less prevalent T2D will become.

Current diagnostic methods for T2D and prediabetes involve blood tests. The most non-invasive method, HbA1c, is a blood test used to measure the proportion of glycated hemoglobin. This metric gives an estimate of the average blood glucose over the last 2-3 months. The next method, the Fasting Blood Glucose test, is slightly more inconvenient. The individual must fast for 8 hours prior to the doctor's visit, then a blood test measures the concentration of remaining glucose in the blood after this period. However, this test can be affected by the circadian rhythm and can vary depending on the time of day. The final, and arguably most diagnostic depiction of glucose homeostasis dysfunction is the Oral Glucose Tolerance Test. This test also requires around 8 hours of fasting beforehand, but once the individual is at the doctor's office they are given a solution of glucose, typically around 75 g. After ingesting the glucose solution and waiting a period of 2 hours, a blood test is performed to measure the concentration of glucose in the blood. This method is the only diagnostic method that takes into account the individual's blood glucose dynamics, as it evaluates how well the individual can manage a large amount of glucose being added to the system. However, it is still just a single value measurement and the blood glucose during the 2 hour wait period is not evaluated [7].

New developments of medical technologies yields the possibility of new diabetic screening methods. For example, in recent years, continuous glucose monitors (CGMs) have become widely available with many pharmacies distributing them over-the-counter. These devices function by placing a small fila-

ment sensor under the skin on the arm or stomach. It then measures the concentration of glucose in the interstitial fluid every few minutes. These readings can be transmitted to a specialized scanner and exported to a computer, and in some cases a cellphone can scan the readings directly [10]. The frequency of measurements and how long the device lasts depends on the brand, for example the FreeStyle Libre will measure glucose every 15 minutes for 2 weeks.

Methods utilizing CGMs for screening and diagnosis are still in development. Perhaps the most well known method is the mean amplitude of glycemic excusion, or MAGE. It is used as an index of glycemic variability and is determined by calculating the mean of the blood glucose values that exceed one standard deviation of the 24 hour mean blood glucose. Higher MAGE scores indicate a higher level of glycemic variability and can be indicative of the lack of glycemic control seen in diabetic individuals [11]. However, the methodology has been criticized as being arbitrary in the choice of one standard deviation, and that the calculation is dependent on the operator when using a graphical approach [12]. Furthermore, MAGE has a very high correlation with the standard deviation of an individual's CGM data (r= 0.96), but is much less efficient and more difficult to calculate [12, 13].

Application of math models to CGM data pose a promising alternative to current methods. The abundance of data easily collected from CGMs provide a pseudo-continuous depiction of blood glucose dynamics. Applying a system of differential equations to this data will allow for a more robust depiction of an individual's glucose control.

Math modelling of the glucose control system has been explored since the early 1960s. The first models were developed as compartment models simulating the glucose-insulin system. One example was a model developed by Victor Bolie in 1960 . Data from previous animal experiments was fit to a 2-equation ordinary differential equation model and extrapolated to give estimates of insulin and glucose dynamics in a human male [14].

Similarly, a study published in 1979 by Richard Bergman fit data obtained by performing intravenous glucose tolerance tests on dogs to seven different differential equation compartment models of the blood glucose system. This article developed a metric denoted the Insulin sensitivity index from the parameter values, which was defined as the "dependence of fractional glucose disappearance on plasma insulin". This metric could be obtained from a single glucose injection, and it was concluded that this metric may have clinical applicability [15].

The glucagon-glucose control system was modelled much later than the insulin-glucose system. One of the first models that incorporated both systems was by Saunders in 1998. Here, the idea of rein control was introduced in the context of the glucose control system. If glucose levels were too high, it would activate the insulin branch of the model to bring levels back to normal. Alternatively if glucose was too low, the glucagon branch would be activated to increase glucose back to normal. This method was analogous to pulling on the reigns of a horse to keep it centered on a set path [16].

Recent developments of the glucose control system involve more comprehensive models. These models involve tens to hundreds of parameters to be fit, but give a more complete depiction of the mechanisms involved in glucose homeostasis. These models do not use a compartment approach, and instead tend to model the actual cell-to-cell interactions of the system. A recent example of this was developed by Masroor in 2019. This model simulates the release of glucagon and insulin from the alpha and beta pancreatic cells respectively. To implement this model with CGM data, 11 parameters would need to be fit to 5 differential equations in order to reproduce measured data [17].

One restriction of the models discussed is that they require measurements of insulin and glucagon in order to yield accurate predictions of blood glucose control. This eliminates the benefits of using a CGM for diagnosis, as blood tests would still be required to obtain these hormone levels. Furthermore, many models require estimates of consumed glucose or consumption of a specific form of food (such as a liquid diet), even recent models developed specifically for use on CGM data [18, 19].

van Veen et. al. developed a single-equation differential model that used a proportional-integral (PI) controller [20]. The details of this particular model will be discussed in the next section, but this particular type of control is common in engineering – particularly in temperature regulation or flight stabilization. It involves two types of control: the proportional control responds to the exact deviation of the controlled metric at that point in time; and the integral control which responds to what has happened in the recent past. This results in different control depending on if the deviation was slow or almost instantaneous. This type of control only requires three inputs - the past and current values of the metric you are attempting to control, the baseline or ideal value of the controlled metric, and how far back in the past you wish to look for the integral response (i.e. the memory of the system). When applying this system to the glucose control system, the baseline value and the memory can be fit to the data, and the only measurements required are the blood glucose concentrations. This effectively eliminates the need for hormone measurements and allows a model to be fit to exclusively CGM data.

1.2 Thesis Objectives

The objective of this thesis is to explore the applicability of the model developed by van Veen et al. [20], both to healthy individuals and to individuals with T2D and prediabetes. Dynamical system analysis will be performed on the model, and we establish the model has a stable equilibrium for constant glucose input and solutions remain bounded for time-dependent input. We further show that the parameters obtained from fitting the model to healthy individual's CGM data across four studies follow a normal or log-normal distribution, and that the parameter results obtained from individual's with type 2 diabetes and prediabetes follow a slightly different distribution. Finally, parameter results were used to construct two biomarkers of diabetic status: a single value biomarker constructed using the standard deviation of the parameters, and a distribution comparison biomarker to compare the overall distribution of parameters for each individual. Both biomarkers can be used to predict diabetic status of type 2 diabetic or prediabetic individuals.

2 Model Introduction

2.1 Model Formulation

The dynamics of blood glucose homeostasis and its regulating feedback system are modelled by a system of coupled differential and integral equations. We assume that there are three components contributing to variations in glucose deviation: 1) Base metabolic rate - the rate that glucose is consumed during rest to maintain basic bodily functions, 2) A negative feedback mechanism that regulates blood glucose concentration as it deviates from normal levels, and 3) an input function that describes the external intake of glucose such as those received by eating a meal. The equation is

$$\frac{\mathrm{d}e}{\mathrm{d}t} = -A_3 - u\phi(e, \bar{e}) + F(t) \tag{1}$$

where e is the excess glucose concentration from some set value $\bar{e}$. The base metabolic rate A_3 is assumed constant, and $F(t)$ models the external glucose sources (i.e. food intake) and sinks (such as vigorous exercise). The control variable u represents the collective effects of the active mechanisms that promote returning blood glucose levels to normal. The aggregate effect is modelled using a proportional-integral strategy and is described by the equation

$$u = A_1 e + A_2 \int_{t'=-\infty}^{t} \lambda \exp^{-\lambda(t-t')} e(t')\mathrm{d}t'. \tag{2}$$

The coefficients of proportional and integral response are A_1 and A_2 respectively, and $1/\lambda$ is the time scale of the delays in the feedback mechanism. Note that regardless of the deviation (increase or decrease) of glucose, the aggregated effect of the controller will act to bring glucose back to baseline levels. Finally, the feedback term ϕ takes a different form for positive and negative deviations e.

For positive deviations (hyperglycemia), the main feedback mechanism involves the excretion of insulin and the uptake of a fraction of the total glucose concentration per time unit. This mechanism is modelled by mass action kinetics, resulting in a quadratic term similar to that used by Bergman [15]. For negative deviations (hypoglycemia), the main feedback mechanism is that of the release of glucagon which, in turn, triggers the release of glucose from the liver. This process we model with a linear term as we consider the supply of glucose from the liver instantaneous and unlimited. The feedback ϕ is defined as

$$\phi(e, \bar{e}) = \max\{e + \bar{e}, \bar{e}\}. \tag{3}$$

2.2 Dynamical System Analysis

Dynamical system analysis will be performed on the aforementioned differential equation system. This will be done to ensure the system behaves as expected at reasonable parameter values. To perform dynamical system analysis, the differential equation system will first be converted from a one dimensional differential equation model to two dimensions. This is done as follows:

For the hyperglycemic model, we differentiate the equation for u, yielding

$\dot{u} = A_1\dot{e} + A_2\lambda e - A_2\lambda^2 \int_{-\infty}^{t} e^{-\lambda(t-t')}e(t')dt'$

Adding $\dot{u}$ to the initial equation for u multiplied by λ:

$\dot{u} + \lambda u = \lambda A_1 e + A_1\dot{e} + A_2\lambda e$

The memory term is now gone, and $\dot{e}$ and $\dot{u}$ can now be represented as:

$\dot{e} = g(u, e)$

$$\dot{u} = -\lambda u + \lambda(A_1 + A_2)e + A_1 g(u, e)$$

Where: $g(u, e) = -A_3 - u(e + \bar{e}) + F(t)$

Using the same process, we can convert the hypoglycemic model to a two dimensional ODE system:

$$\dot{e} = g(u, e)$$

$$\dot{u} = -\lambda u + \lambda(A_1 + A_2)e + A_1 g(u, e)$$

Where: $g(u, e) = -A_3 - A_4 u + F(t)$

The analysis will be performed assuming a constant input, such that $F(t) = C$.

2.2.1 Fixed Point Classification of Hypoglycemic Model

The equations for the hypoglycemic model are characterized by:

$$\begin{aligned}
\dot{e} &= -A_3 - u - C \\
\dot{u} &= -\lambda u + \lambda(A_1 + A_2)e + A_1 \dot{e} \\
&= -\lambda u + \lambda(A_1 + A_2)e - A_1 A_3 - A_1 u - A_1 C
\end{aligned}$$

We can find the nullclines of the system by setting both equations above equal to zero. Starting with the $\dot{e}$ nullcline:

$$\begin{aligned}
0 &= -A_3 - u - C \\
u &= -A_3 + C
\end{aligned}$$

Since all parameters are greater than zero, the $\dot{e}$ nullcline will always be a horizontal line below the e axis. Continuing with the $\dot{u}$ nullcline:

$$0 = -\lambda u + \lambda(A_1 + A_2)e - A_1A_3 - A_1u - A_1C$$

$$\lambda u + A_1u = \lambda(A_1 + A_2)e - A_1(A_3 + C)$$

$$u = \frac{\lambda(A_1 + A_2)e - A_1(A_3 + C)}{\lambda + A_1}$$

In order to solve for the fixed points, we can find the intersections of the nullclines. Note, at the intersection, $\dot{e} = 0$ and the nullcline for $\dot{u}$ simplifies to:

$$u = (A_1 + A_2)e$$

Substituting the $\dot{e}$ nullcline in for u:

$$-A_3 + C = (A_1 + A_2)e$$

$$e^* = -\frac{A_3 + C}{A_1 + A_2}$$

Since all parameters are greater than zero, the e value of the fixed point will always be negative. We already know the value of u from the $\dot{e}$ nullcline, so our fixed point, (e^*, u^*) will be at $(-\frac{A_3+C}{A_1+A_2}, -A_3+C)$, which will always lie in the third quadrant.

We can classify the fixed point using the Jacobian of the system.

$$J = \begin{bmatrix} 0 & -A_4 \\ \lambda(A_1 + A_2) & -\lambda - A_1A_4 \end{bmatrix}$$

The trace of the matrix, $\tau(J)$, is equal to $-\lambda - A_1A_4$. The determinant of the matrix, $\triangle$ is equal to $A_4\lambda(A_1 + A_2)$. Given that all parameters are greater than zero, $\tau(J)$ will always be negative and $\triangle$ will

always be positive. Looking at $\tau^2 - 4\triangle$, it is positive when $A_2 < \frac{(\lambda+A_1A_4)^2}{4A_4\lambda} - A_1$ and negative when $A_2 > \frac{(\lambda+A_1A_4)^2}{4A_4\lambda} - A_1$. This indicates that when $A_2 < \frac{(\lambda+A_1A_4)^2}{4A_4\lambda} - A_1$, the fixed point is a stable node. When $A_2 > \frac{(\lambda+A_1A_4)^2}{4A_4\lambda} - A_1$, the fixed point is a stable spiral.

Looking at the condition in which $A_2 = \frac{(\lambda+A_1A_4)^2}{4A_4\lambda} - A_1$, we have a repeated eigenvalue of $-\lambda - A_1A_4$. Solving for the eigenvectors using ϵ to denote the eigenvalues:

$$J\mathbf{x} = \epsilon\mathbf{x}$$

$$\begin{bmatrix} 0 & -A_4 \\ \lambda(A_1 + A_2) & -\lambda - A_1A_4 \end{bmatrix} \begin{bmatrix} x_1 \\ x_2 \end{bmatrix} = (-\lambda - A_1A_4) \begin{bmatrix} x_1 \\ x_2 \end{bmatrix}$$

Multiplying out the left and right hand sides of the equation, we get:

$$-A_4x_2 = (-\lambda - A_1A_4)x_1$$

$$\lambda(A_1 + A_2)x_1 + (-\lambda - A_1A_4)x_2 = (-\lambda - A_1A_4)x_2$$

After solving for x_1 and x_2, we obtain the two linearly independent eigenvectors $\begin{bmatrix} 1 \\ \lambda + A_1 \end{bmatrix}$ and $\begin{bmatrix} 0 \\ 1 \end{bmatrix}$. Thus, the fixed point when $A_2 = \frac{(\lambda+A_1A_4)^2}{4A_4\lambda} - A_1$ is a stable star.

No bifurcations occur in the hypoglycemic system.

We can also analyze the dynamics of the phase space by calculating the nullclines and direction field of the system. Setting $\dot{e}$ equal to zero, we get the $\dot{e}$ nullcline $0 = -A_3 - A_4u - C$, or $u = -A_3 - C$. Setting $\dot{u}$ equal to zero, we get the $\dot{u}$ nullcline $0 = -\lambda u + \lambda(A_1 + A_2)e - A_1A_3 - A_1A_4u - A_1C$, or $u = \frac{\lambda(A_1+A_2)e - A_1(A_3+C)}{\lambda+A_1}$

Calculating the directions the of trajectories along each nullcline:

For the $\dot{e}$ nullcline, $\dot{u} = -\lambda u + \lambda(A_1 + A_2)e$ on the nullcline, and u is a constant negative value at $-A_3 - C$. Substituting this into $\dot{u}$, we get $\dot{u} = \lambda(A_1 + C + (A_1 + A_2)e)$. When $e < -A_3 - C$ (i.e. less than the e value at the fixed point), $\dot{u}$ is negative and the flow will be down. When e is greater than the e value at the fixed point, $\dot{u}$ is positive and the flow will be up.

For the $\dot{u}$ nullcline, for any u greater than the value of u at the fixed point (i.e. $-A_3 - C$, $\dot{e}$ will be negative and flow will be to the left. For any u less than the value of u at the fixed point, $\dot{e}$ will be negative and the flow will be to the left.

2.2.2 Fixed Point Classification of Hyperglycemic Model

The equations for the hyperglycemic model are reflected as:

$$\begin{aligned}
\dot{e} &= -A_3 - u(e + \bar{e}) + C \\
\dot{u} &= -\lambda u + \lambda(A_1 + A_2)e + A_1\dot{e} \\
&= -\lambda u + \lambda(A_1 + A_2)e - A_1A_3 - A_1u(e + \bar{e}) + A_1C
\end{aligned}$$

We can solve for the nullclines by setting both equations equal to zero.

$$\begin{aligned}
\dot{e} = 0 &= -A_3 - u(e + \bar{e}) + C \\
u &= \frac{C - A_3}{(e + \bar{e})} \qquad \text{(Equation for the } \dot{e} \text{ nullcline)}
\end{aligned}$$

$$\begin{aligned}
\dot{u} = 0 &= -\lambda u + \lambda(A_1 + A_2)e - A_1A_3 - A_1u(e + \bar{e}) + A_1C \\
u &= \frac{\lambda(A_1 + A_2)e + A_1(C - A_3)}{\lambda + A_1(e + \bar{e})} \qquad \text{(Equation for the } \dot{u} \text{ nullcline)}
\end{aligned}$$

To solve for the fixed points, we can just solve for the intersection of the nullclines. However, at the fixed points, $\dot{e} = 0$, and $\dot{u} = -\lambda u + \lambda(A_1 + A_2)e$. Setting this equation equal to zero, we obtain

$u^* = (A_1 + A_2)e^*$. Substituting this into the $\dot{e}$ nullcline, we get:

$$\frac{C - A_3}{e * + \bar{e}} = (A_1 + A_2)e*$$
$$(e^*)^2 + \bar{e}e^* + \frac{A_3 - C}{A_1 + A_2} = 0$$

Using the quadratic formula, we can solve for the value of e at the fixed point, e^*

$$e^* = \frac{-\bar{e} \pm \sqrt{(\bar{e})^2 - 4\frac{A_3 - C}{A_1 + A_2}}}{2}$$

Using $u^* = (A_1 + A_2)e^*$, we obtain:

$$u^* = (A_1 + A_2)\frac{-\bar{e} \pm \sqrt{(\bar{e})^2 - 4\frac{A_3 - C}{A_1 + A_2}}}{2}$$

By observation, we can see that there are two fixed points when $(\bar{e})^2 - 4\frac{A_3 - C}{A_1 + A_2} > 0$, 1 fixed point when $(\bar{e})^2 - 4\frac{A_3 - C}{A_1 + A_2} = 0$, and no fixed points when $(\bar{e})^2 - 4\frac{A_3 - C}{A_1 + A_2} < 0$. Thus, a saddle node bifurcation occurs when $(\bar{e})^2 - 4\frac{A_3 - C}{A_1 + A_2} = 0$, or when $C = -(A_1 + A_2)\frac{(\bar{e})^2}{4} + A_3$.

We can classify the fixed points of the system using the Jacobian matrix, defined below:

$$J = \begin{bmatrix} -u & -(e + \bar{e}) \\ \lambda(A_1 + A_2) - A_1 u & -\lambda - A_1(e + \bar{e}) \end{bmatrix}$$

Calculating the determinant:

$$\begin{aligned} \triangle &= \lambda u + A_1 u(e + \bar{e}) - [-\lambda(A_1 + A_2)(e + \bar{e}) + A_1 u(e + \bar{e})] \\ &= \lambda u + \lambda(A_1 + A_2)(e + \bar{e}) \end{aligned}$$

At the fixed points, $u^* = (A_1 + A_2)e^*$, and

$$\begin{aligned}\triangle &= \lambda u^* + \lambda(A_1 + A_2)(e^* + \bar{e}) \\ &= \lambda(A_1 + A_2)e^* + \lambda(A_1 + A_2)(e^* + \bar{e}) \\ &= \lambda(A_1 + A_2)(2e^* + \bar{e})\end{aligned}$$

Starting with the fixed point $(e_1^*, u_1^*) = \left(\frac{-\bar{e}-\sqrt{(\bar{e})^2-4\frac{A_3-C}{A_1+A_2}}}{2}, (A_1 + A_2)\frac{-\bar{e}-\sqrt{(\bar{e})^2-4\frac{A_3-C}{A_1+A_2}}}{2}\right)$:

$$\begin{aligned}\triangle &= \lambda(A_1 + A_2)\left(2\left(\frac{-\bar{e} - \sqrt{(\bar{e})^2 - 4\frac{A_3-C}{A_1+A_2}}}{2}\right) + \bar{e}\right) \\ &= \lambda(A_1 + A_2)\left(-\bar{e} - \sqrt{(\bar{e})^2 - 4\frac{A_3 - C}{A_1 + A_2}} + \bar{e}\right) \\ &= \lambda(A_1 + A_2)\left(-\sqrt{(\bar{e})^2 - 4\frac{A_3 - C}{A_1 + A_2}}\right) \\ &= -\lambda(A_1 + A_2)\sqrt{(\bar{e})^2 - 4\frac{A_3 - C}{A_1 + A_2}}\end{aligned}$$

By definition, $\lambda, A_1, A_2 > 0$. Assuming that $(\bar{e})^2 - 4\frac{A_3-C}{A_1+A_2} > 0$ (i.e. the system is not at the bifurcation point), the determinant will always be negative and the fixed point will always be a saddle point.

At the fixed point $(e_2^*, u_2^*) = \left(\frac{-\bar{e}+\sqrt{(\bar{e})^2-4\frac{A_3-C}{A_1+A_2}}}{2}, (A_1 + A_2)\frac{-\bar{e}+\sqrt{(\bar{e})^2-4\frac{A_3-C}{A_1+A_2}}}{2}\right)$:

$$\begin{aligned}\triangle &= \lambda(A_1 + A_2)(2e^* + \bar{e}) \\ &= \lambda(A_1 + A_2)\left(2\left(\frac{-\bar{e} + \sqrt{(\bar{e})^2 - 4\frac{A_3-C}{A_1+A_2}}}{2}\right) + \bar{e}\right) \\ &= \lambda(A_1 + A_2)\sqrt{(\bar{e})^2 - 4\frac{A_3 - C}{A_1 + A_2}}\end{aligned}$$

Assuming $(\bar{e})^2 - 4\frac{A_3-C}{A_1+A_2} > 0$ (i.e. the system is not at the bifurcation point) and $\lambda, A_1, A_2 > 0$, the determinant will always be positive. Calculating the trace of the Jacobian:

$$\tau = -u - \lambda - A_1(e + \bar{e})$$

At the fixed point, $u^* = (A_1 + A_2)e^*$

$$\begin{aligned}
\tau &= -(A_1 + A_2)e^* - \lambda - A_1(e^* + \bar{e}) \\
&= -A_1e^* - A_2e^* - \lambda - A_1e^* - A_1\bar{e} \\
&= -2A_1e^* - A_2e^* - \lambda - A_1\bar{e} \\
&= -2A_1\left(\frac{-\bar{e} + \sqrt{(\bar{e})^2 - 4\frac{A_3-C}{A_1+A_2}}}{2}\right) - A_2\left(\frac{-\bar{e} + \sqrt{(\bar{e})^2 - 4\frac{A_3-C}{A_1+A_2}}}{2}\right) - \lambda - A_1\bar{e} \\
&= A_1\bar{e} - A_1\sqrt{(\bar{e})^2 - 4\frac{A_3 - C}{A_1 + A_2}} - A_2\left(\frac{-\bar{e} + \sqrt{(\bar{e})^2 - 4\frac{A_3-C}{A_1+A_2}}}{2}\right) - \lambda - A_1\bar{e} \\
&= -A_1\sqrt{(\bar{e})^2 - 4\frac{A_3 - C}{A_1 + A_2}} - A_2\left(\frac{-\bar{e} + \sqrt{(\bar{e})^2 - 4\frac{A_3-C}{A_1+A_2}}}{2}\right) - \lambda \\
&= \frac{A_2\bar{e}}{2} - (A_1 + \frac{A_2}{2})\sqrt{(\bar{e})^2 - 4\frac{A_3 - C}{A_1 + A_2}} - \lambda
\end{aligned}$$

Calculating $\tau^2 - 4\triangle$:

$$\begin{aligned}
\tau^2 - 4\triangle &= \left(\frac{A_2\bar{e}}{2} - (A_1 + \frac{A_2}{2})\sqrt{(\bar{e})^2 - 4\frac{A_3 - C}{A_1 + A_2}} - \lambda\right)^2 - 4\left(\lambda(A_1 + A_2)\sqrt{(\bar{e})^2 - 4\frac{A_3 - C}{A_1 + A_2}}\right) \\
&= \left(\frac{A_2\bar{e}}{2}\right)^2 + \left((A_1 + \frac{A_2}{2})\sqrt{(\bar{e})^2 - 4\frac{A_3 - C}{A_1 + A_2}}\right)^2 + (\lambda)^2 - 2\lambda\frac{A_2\bar{e}}{2} \\
&+ 2\lambda\left((A_1 + \frac{A_2}{2})\sqrt{(\bar{e})^2 - 4\frac{A_3 - C}{A_1 + A_2}}\right) - 2\frac{A_2\bar{e}}{2}\left((A_1 + \frac{A_2}{2})\sqrt{(\bar{e})^2 - 4\frac{A_3 - C}{A_1 + A_2}}\right) \\
&- 4\lambda(A_1 + A_2)\sqrt{(\bar{e})^2 - 4\frac{A_3 - C}{A_1 + A_2}} \\
&= \left(\frac{A_2\bar{e}}{2}\right)^2 + (A_1 + \frac{A_2}{2})^2\left((\bar{e})^2 - 4\frac{A_3 - C}{A_1 + A_2}\right) + \lambda^2 - \lambda A_2\bar{e} \\
&+ 2\lambda(A_1 + \frac{A_2}{2})\sqrt{(\bar{e})^2 - 4\frac{A_3 - C}{A_1 + A_2}} - A_2\bar{e}(A_1 + \frac{A_2}{2})\sqrt{(\bar{e})^2 - 4\frac{A_3 - C}{A_1 + A_2}} \\
&- 4\lambda(A_1 + A_2)\sqrt{(\bar{e})^2 - 4\frac{A_3 - C}{A_1 + A_2}} \\
&= \left(\frac{A_2\bar{e}}{2}\right)^2 + (A_1 + \frac{A_2}{2})^2\left((\bar{e})^2 - 4\frac{A_3 - C}{A_1 + A_2}\right) + \lambda^2 - \lambda A_2\bar{e} \\
&+ (2\lambda A_1 + \lambda A_2 - \bar{e}A_1A_2 - \bar{e}\frac{A_2^2}{2} - 4\lambda A_1 - 4\lambda A_2)\sqrt{(\bar{e})^2 - 4\frac{A_3 - C}{A_1 + A_2}} \\
&= \left(\frac{A_2\bar{e}}{2}\right)^2 + (A_1 + \frac{A_2}{2})^2\left((\bar{e})^2 - 4\frac{A_3 - C}{A_1 + A_2}\right) + \lambda^2 - \lambda A_2\bar{e} \\
&+ (-\bar{e}A_1A_2 - \frac{\bar{e}A_2^2}{2} - 2\lambda A_1 - 3\lambda A_2)\sqrt{(\bar{e})^2 - 4\frac{A_3 - C}{A_1 + A_2}} \\
&= \left(\frac{A_2\bar{e}}{2}\right)^2 + (A_1 + \frac{A_2}{2})^2\left((\bar{e})^2 - 4\frac{A_3 - C}{A_1 + A_2}\right) + \lambda^2 - \lambda A_2\bar{e} \\
&- (\bar{e}A_1A_2 + \frac{\bar{e}A_2^2}{2} + 2\lambda A_1 + 3\lambda A_2)\sqrt{(\bar{e})^2 - 4\frac{A_3 - C}{A_1 + A_2}}
\end{aligned}$$

This will be negative if:

$$\begin{aligned}
&\lambda A_2\bar{e} + (\bar{e}A_1A_2 + \frac{\bar{e}A_2^2}{2} + 2\lambda A_1 + 3\lambda A_2)\sqrt{(\bar{e})^2 - 4\frac{A_3 - C}{A_1 + A_2}} \\
&\qquad > \left(\frac{A_2\bar{e}}{2}\right)^2 + \lambda^2 + (A_1 + \frac{A_2}{2})^2\left((\bar{e})^2 - 4\frac{A_3 - C}{A_1 + A_2}\right)
\end{aligned}$$

Or, if the negative terms in $\tau^2 - 4\triangle$ are greater than the positive terms. Consequently, it will be positive if

$$\begin{aligned}\lambda A_2\bar{e} + (\bar{e}A_1A_2 + \frac{\bar{e}A_2^2}{2} + 2\lambda A_1 + 3\lambda A_2)\sqrt{(\bar{e})^2 - 4\frac{A_3 - C}{A_1 + A_2}} \\ < \left(\frac{A_2\bar{e}}{2}\right)^2 + \lambda^2 + (A_1 + \frac{A_2}{2})^2\left((\bar{e})^2 - 4\frac{A_3 - C}{A_1 + A_2}\right)\end{aligned}$$

Or, if the negative terms in $\tau^2 - 4\triangle$ are less than the positive terms. Unfortunately, this is as far as the model can be reduced, so exact fixed point behaviour (i.e. node vs spiral) can only be calculated when the parameters are known.

If $C \geq A_3$, $\sqrt{(\bar{e})^2 - 4\frac{A_3 - C}{A_1 + A_2}} \geq \bar{e}$, $(\bar{e})^2 - 4\frac{A_3 - C}{A_1 + A_2} \geq \bar{e}^2$. Recalculating the trace:

$$\begin{aligned}\tau &= \frac{A_2\bar{e}}{2} - (A_1 + \frac{A_2}{2})\sqrt{(\bar{e})^2 - 4\frac{A_3 - C}{A_1 + A_2}} - \lambda \\ \tau &\leq \frac{A_2\bar{e}}{2} - A_1\bar{e} - \frac{A_2\bar{e}}{2} - \lambda \\ \tau &\leq -A_1\bar{e} - \lambda\end{aligned}$$

Therefore, if the input is greater than A_3, the fixed point will be stable, since $A_1, \bar{e}, \lambda > 0$. We know that the determinant is always positive, so the fixed point at (e_2^*, u_2^*) when $C \geq A_3$ will either be a stable spiral or a stable node.

2.2.3 Global Stability

In a recent paper, it was determined that a trapping region can be constructed to show global stability of the dynamical system using a Lyapunav function, $L(t)$ [21]. It was shown that solutions to the differential equation system with constant input $G = -A_3 + C$ will eventually enter the interior of the curve $L = K$

and remain there. The minimal value of K is bounded from above by

$$K_- = \frac{1}{8A_1\lambda\bar{e}^2}\Big(\Big[2\bar{e}^2\sqrt{A_1A_2} + 4\bar{e}\lambda\Big] \sqrt{A_1A_2\bar{e}^4 + [A_1\bar{e}^2 + G]^2} \\ + A_1(A_1 + 2A_2)\bar{e}^4 - 4A_1\bar{e}^3\lambda + 2A_1G\bar{e}^2 + 4G\bar{e}\lambda + G^2\Big) \tag{4}$$

if $G \leq -A_2\bar{e}^2/4$ and by

$$K_+ = \frac{1}{8A_1\lambda\bar{e}^2}\Big(2\sqrt{A_1A_2}\bar{e}^2\sqrt{A_1A_2\bar{e}^4 + [A_1\bar{e}^2 + G]^2} + (A_1\bar{e}^2 + G)^2 \\ + 4\lambda\bar{e}^2\sqrt{A_1[A_1 + A_2]\bar{e}^2 + 4A_1G} + 2A_1A_2\bar{e}^4 - 4A_1\bar{e}^3\lambda\Big) \tag{5}$$

if $G > -A_2\bar{e}^2/4$.

Using the above result, boundedness of solutions with variable input, $G(t) = -A_3 + F(t)$, can also be determined. Assuming G is bounded, i.e. $G_{\min} \leq G(t) \leq G_{\max}$ for $t \in [0, \infty)$ and letting $G_{\max} > 0$, it was determined that solutions to to the system of equations eventually enter the interior of the curve $L = K$ and remain there. The constant K is given by

$$K = \max\{K_-(G_{\min}), K_+(G_{\max})\} \tag{6}$$

3 Model Application

3.1 Methods

Figure 1: **Study Flow Chart**

Results were analyzed from data obtained from four different studies: 1) a study conducted by researchers at Stanford University ($N = 57$), referred to in this thesis as the Stanford Study [22], 2) a pilot study conducted by Klick Labs in Toronto ($N = 42$) [23], referred to in this thesis as the Klick Pilot Study, 3) a followup study conducted by Klick Labs on individuals living in India ($N = 146$), referred to in this thesis as the Klick Followup Study 1 [24], and 4) a larger followup study conducted by Klick Labs on individuals living in India ($N = 277$), referred to as the Klick Followup Study 2 [25].

In the studies conducted by Klick Labs, participants were fitted with a Freestyle Libre continuous glucose monitor device. Blood glucose concentrations were automatically recorded every 15 minutes for 2 weeks, resulting in approximately 1400 data points per person. In the Stanford Study, participants were fitted with a Dexcom G4 CGM device. Blood glucose concentrations were automatically recorded every 5 minutes for a minimum of 2 weeks up to a maximum of 4 weeks. The protocol for the Stanford Study is described further in the paper *Glucotypes reveal new patterns of glucose dysregulation* [22]. All participants in the Klick pilot and follow-up studies gave informed consent to complete the survey, and both studies received full ethics clearance from Advarra IRB Service and from Ontario Tech University's ethic review board.

Glucose baselines are calculated by taking averaging the glucose values of all the local minima from the entire time series. The justification behind this method is that the glucose levels seem to fluctuate

more around the baseline, as small glucose deviations are brought back to normal levels through the insulin-glucagon system. This is a simple alternative to just taking the mean of all glucose levels over the entire time series. Taking the average glucose concentration typically results in a baseline that is higher than what is expected by observing the glucose time series, and may result in some glucose fluctuations to be lost during peak selection. A comparison of the two methods can be seen in Figure **??**.

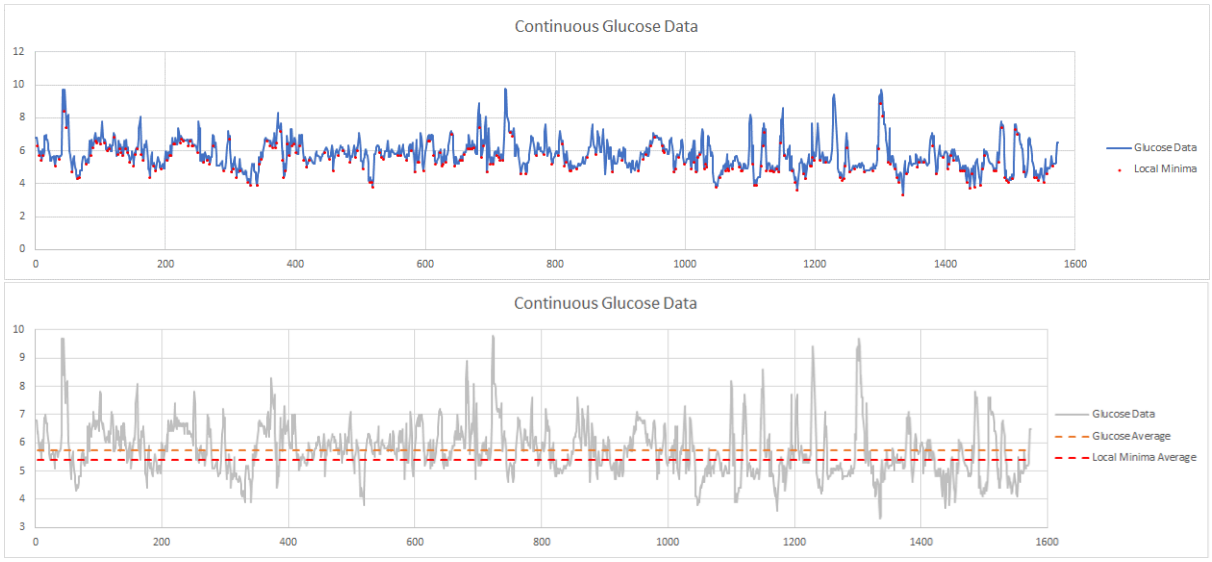

Figure 2: **Illustration of Baseline Calculation**

After the baseline glucose level is calculated from a time series, positive and negative glucose deviations (denoted "peaks" and "troughs" respectively) were extracted in order to apply the model. A discrete Gaussian filter was applied to the entire time series, using a standard deviation of one 15 minute interval. The first derivatives were calculated along the entire time series for the smoothed glucose data using a discrete difference method. Peaks were defined as follows:

- The peak maximum occurs where the first derivative of the smoothed data changes from positive to negative
- The peak endpoints occur where the first derivative changes from negative to positive

Selected peaks were then mapped back to corresponding time points in the raw glucose data. From this

point, they were filtered using the following criteria:

- Peaks must be greater than or equal to one hour, or four data points. This is an attempt to reduce any peaks that are a result of instrument noise rather than increasing glucose levels
- The peak maximum must be greater than the baseline plus one standard deviation of the glucose data over the entire time series.
- The peak endpoints must be within the range [baseline $\pm$ one glucose standard deviation of the time series]

At this point, the peaks were ready to be fed into the gradient descent framework and be fit to the model. Each peak and trough extracted were fitted against the proposed model by minimizing the function

$$E = \frac{\sum_{i=1}^{n} (\tilde{e}(t_i) - e(t_i))^2}{\sum_{i=1}^{n} \tilde{e}(t_i)^2} \tag{7}$$

where $\tilde{e}(t)$ is the raw glucose deviation from baseline, and n is the number of recorded points for a particular peak or trough. The base metabolic rate A_3 is assumed constant as all individuals in the study are considered healthy. The external input function $F(t)$ is modelled using a Gaussian function with a variable amplitude and variance, and the center was set to be 15 minutes (1 time interval) before the glucose peak optimum. During hyperglycemia, this agrees reasonably well with data measured in vitro [**?**]. In hypoglycemic cases, $F(t)$ takes the same form but with a negative amplitude to model the source causing a drop in blood glucose levels. $\bar{e}$ is set to the minimum value of the selected peak for hyperglycemic fittings, and the maximum value of the selected peak for hypoglycemic model fitting. The integral term of the control variable was numerically approximated via the midpoint rule, and forward Euler method was used for time stepping. A schematic of the gradient descent implementation, adapted from [20], is shown in Figure 3.

Different peak extraction thresholds were explored, including evaluating the baseline plus or minus one

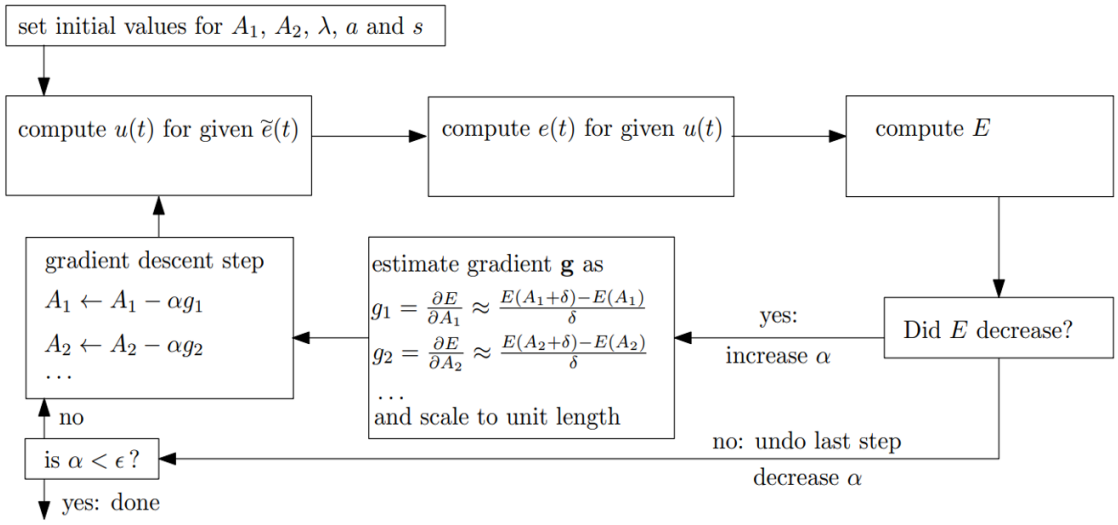

Figure 3: **Gradient Descent Implementation for Parameter Fitting.** Starting at the top left, we set the initial values parameters of A_1, A_2, λ, a, and s, where a and s are the amplitude and standard deviation of the Gaussian input function, $F(t)$. The initial step size is set to $\alpha = 1$. We then compute the model output $e(t)$ and its difference from the representative peak $\tilde{e}$. The gradient of the function E (calculated from Equation 7) is approximated by finite differencing with a small constant δ making a 1% variation of the parameter. A gradient descent step of size α is then taken. If E increases from one iteration to the next, the step is rejected and α is decreased. When α is smaller than a pre-set threshold $\epsilon < 10^{12}$, the algorithm has converged. Adapted from [20].

half standard deviation for the endpoint ranges, or having different ranges for the left and right endpoints. Using other extraction criteria occasionally resulted in extracted values that did not resemble the desired peak shape. For instance, there were occasionally peaks extracted that did not include the entire increase and subsequent decrease back to baseline. In these cases, the beginning or end data points were left out, leaving the extracted peak lopsided compared to the actual peak in the CGM data. Ultimately it was determined that the current criteria was the most robust in the peak selection, yielding the highest number of peaks with the proper shape.

3.2 Application to Healthy Individuals

The proposed model was initially validated using glucose data collected from individuals who are considered healthy based on the diabetic diagnostic metrics oral glucose tolerance test (OGTT) and the measure of glycated haemoglobin (HbA1c).

Individuals selected for the study were considered healthy using the guidelines provided by the American Diabetes Association, where A1c levels are below 5.7%, FBG below 100 mg/dL, and OGTT below 140 mg/dL. In addition, the selected participants are not known to be diagnosed with any medical condition where medication may interfere with the subjects' blood glucose regulation. In the Klick Followup 2 study, only HbA1c measurements were taken (no OGTT), so they were classified exclusively using the threshold for HbA1c. The resultant number of participants was $N = 224$, where $N = 36$ individuals were from the Stanford Study, $N = 42$ individuals were from the Klick Pilot Study, $N = 57$ were from the Klick Followup Study 1, and $N = 89$ were from the Klick Followup Study 2.

Upon extracting the peaks and troughs of individual CGM data, the peaks and troughs of individuals were fitted to the model with a fitting error of 0.3028 ± 0.6297 ($E_{\max} = 3.7545$) and 0.1159 ± 0.1780 ($E_{\max} = 1.2578$) respectively, as defined in Eq 7. In a small number of cases ($< 0.5\%$ of all selected peaks), fitting error was comparatively high due to the shape of the selected peaks. In these instances,

two or more smaller peaks were combined together into one automatically selected peak, resulting in a glucose deviation that was multi-modal. An example multi-modal peak can be seen in Fig 6. Two of each representative peaks and troughs are shown in Fig 4 and Fig 5 with similar error to the mean. This demonstrates that our model is able to reproduce glucose levels of healthy individuals with good agreement to real world measurements.

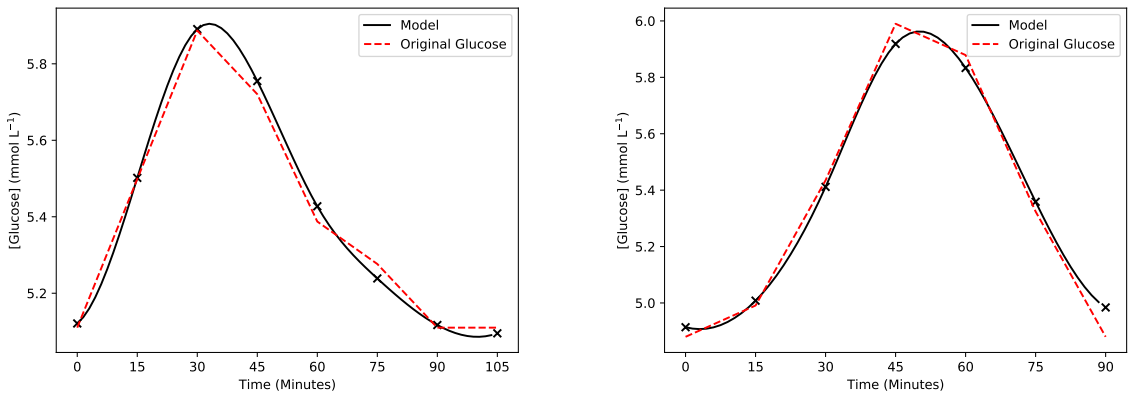

Figure 4: **Example results of the hyperglycemic model.** The original glucose data is represented by the red dashed lines. The set of black crosses is the model glucose output, and the black curve is the cubic spline interpolation of the model outputs.

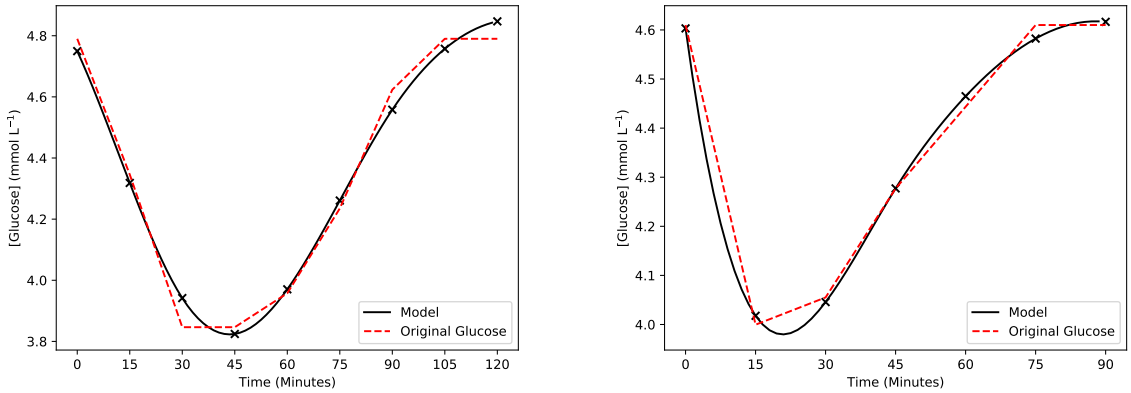

Figure 5: **Example results of the hypoglycemic model.** The original glucose data is represented by the red dashed lines. The set of black crosses is the model glucose output, and the black curve is the cubic spline interpolation of the model outputs.

Figure 1 outlines the range of parameter values across each of the three datasets. In each study, the mean of each parameter value fall within 15% of the overall mean. In addition, the largest coefficient of variation is 0.3402 (Hyperglycemic, A_1, Klick Follow-up), indicating low variances across all model

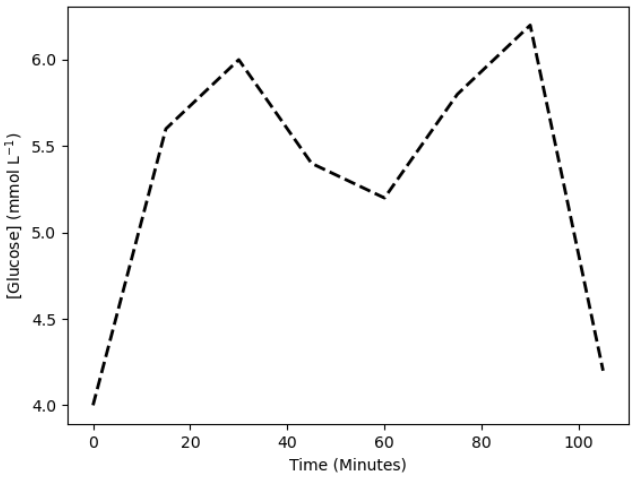

Figure 6: **Representative Bimodal Peak.** The original glucose data is represented by the black dashed lines.

parameters (seen in Table 2). This suggests that the distributions of A_1, A_2, and λ are independent from the source of data. From this it can be concluded that the model results are consistent regardless of the presence of intangibles such as cultural and demographic differences. Due to our peak/trough selection method and length differences in CGM data, the number of peaks/troughs extracted vary between different individuals. The means of A_1 and A_2 for each individual were computed (via bootstrapping) to compensate for this inconsistency. We observed that the means of A_1 and A_2 result in a clustering behaviour, demonstrated graphically in Figure 7.

The parameters A_1, A_2, and λ for all selected peaks for each individual were bootstrapped to derive an estimation of the distribution of parameter values. A description of the bootstrap average calculation can be found in Appendix A. Their respective distributions were tested for normality using the Shapiro-Wilk test with 0.05 as the critical p-value. The distributions of parameter values and Gaussian overlays are shown in Figures 8 and 9 respectively, as well as the corresponding Q–Q Plots. If the data falls directly on the diagonal line in a Q-Q plot, the distribution is normal. However, if the data is U-shaped compared to the diagonal line, the distribution is skewed, and data deviating in opposite directions from the line at the ends correspond to heavier or lighter tails. The data suggests that all parameters follow a normal

distribution except hypoglycemic λ. Upon further investigation, we discovered that λ falls under a log-normal distribution. This was confirmed by the performing the Shapiro-Wilk test on $\log \lambda$, resulting in a p-value of 0.419. The results of the Shapiro-Wilk test are included in 1.

The experiments were performed on a HP EliteBook x360 1030 G4 laptop, with an Intel Core i7-8665U at 1.9GHz, and 16.0 GB of system memory. Depending on the number of peaks/troughs extracted, the tests required five to ten minutes to analyze the time series of an individual. However, the vast majority (90%+) of single peaks/troughs require less than one second to compute their corresponding parameter values. We can, therefore, obtain results in real time whenever peaks/troughs are detected by wearable glucose monitoring sensors. Our data supports that the parameters of our model are normally distributed, with the exception λ for hypoglycemia, which falls under a log-normal distribution. This suggests that the model parameters remain fairly structured among healthy individuals regardless of the source of the data. We observed that all three parameters were noticeably different in value between hyperglycemic and hypoglycemic cases. In particular, parameter values for hyperglycemia are lower than that of hypoglycemia. This was expected because the control systems modelling hyperglycemic/hypoglycemic cases are fundamentally different, mathematically speaking. At sufficiently large deviations, the quadratic control of the hyperglycemic model provides a much stronger feedback mechanism compared to the linear control found in the hypoglycemic counterpart. Therefore, lower parameter values are needed for the hyperglycemic model to achieve similar levels of feedback impact. As we extend our data to include pre-diabetic and diabetic individuals for future studies, we expect values for A_1 and A_2 to decrease as individual's state of health worsens. In extreme cases, we suspect that the structure of the model parameters will quickly deteriorate. Should these claims prove to be correct, a variation and/or combination of A_1 and A_2 may be used as potential biomarkers for early detection of glucose homeostatic dysfunction of individuals.

		Klick Pilot	Klick Follow-up	Stanford	Overall	p-value
Hyperglycemic	A_1	0.0077 ± 0.0020	0.0074 ± 0.0025	0.0064 ± 0.0019	0.0073 ± 0.0022	0.180
	A_2	0.0029 ± 0.0009	0.0037 ± 0.0007	0.0028 ± 0.0009	0.0033 ± 0.0009	0.135
	λ	0.0290 ± 0.0011	0.0293 ± 0.0012	0.0286 ± 0.0009	0.0289 ± 0.0009	0.175
Hypoglycemic	A_1	0.0227 ± 0.0036	0.0197 ± 0.0053	0.0217 ± 0.0037	0.0208 ± 0.0048	0.221
	A_2	0.0364 ± 0.0041	0.0364 ± 0.0037	0.0319 ± 0.0032	0.0354 ± 0.0041	0.143
	λ	0.0417 ± 0.00568	0.0391 ± 0.0052	0.0363 ± 0.0055	0.0395 ± 0.0059	0.022
	$\log \lambda$	-1.3648 ± 0.0548	-1.4112 ± 0.0591	-1.4443 ± 0.0629	-1.4078 ± 0.0649	0.419

Table 1: **Ranges of model parameters.**
Model parameter ranges for hyperglycemic and hypoglycemic cases with their respectively p-values of the Shapiro-Wilk test for normality. The null-hypothesis H_0 states that the model parameters are normally distributed. The decision to reject or not reject H_0 is based on a critical p-value of 0.05.

		Klick Pilot	Klick Follow-up	Stanford	Overall
Hyperglycemic	A_1	0.260	0.340	0.297	0.301
	A_2	0.310	0.189	0.321	0.273
	λ	0.038	0.042	0.031	0.031
Hypoglycemic	A_1	0.159	0.269	0.171	0.231
	A_2	0.113	0.102	0.100	0.116
	λ	0.136	0.133	0.152	0.149

Table 2: **Coefficient of Variation of Model Parameters.**
Coefficient of variation is calculated by dividing the standard deviation of a model parameter by the mean of the same parameter.

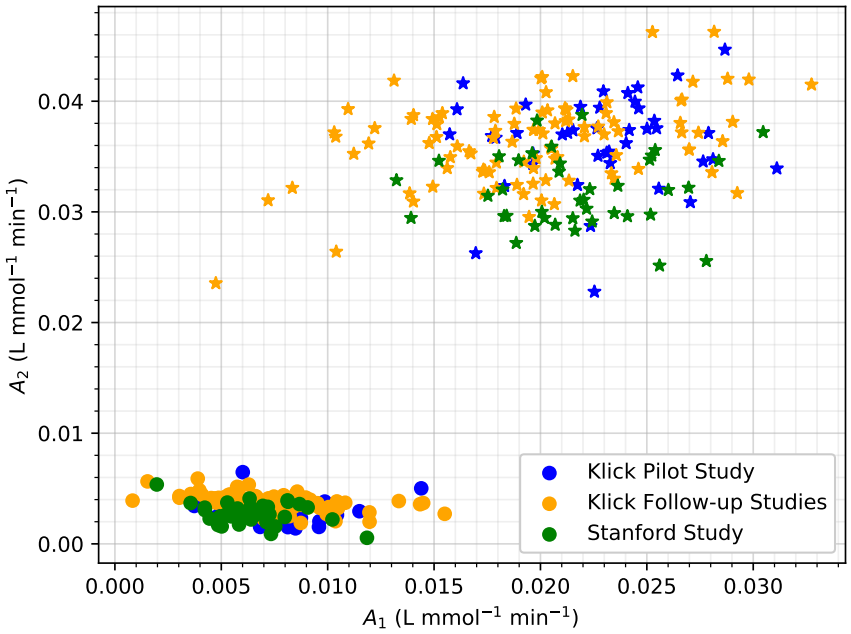

Figure 7: **Comparison of model parameter clustering between hyperglycemic and hypoglycemic episodes**Mean (by subject) model parameter values for peaks and troughs found in hyperglycemic and hypoglycemic cases respectively. Parameter values for hyperglycemic cases are depicted by the circle markers, and in contrast, star markers represent parameter values for hypoglycemic cases. The units of A_1 and A_2 are both in litre/(min $\times$ mmol).

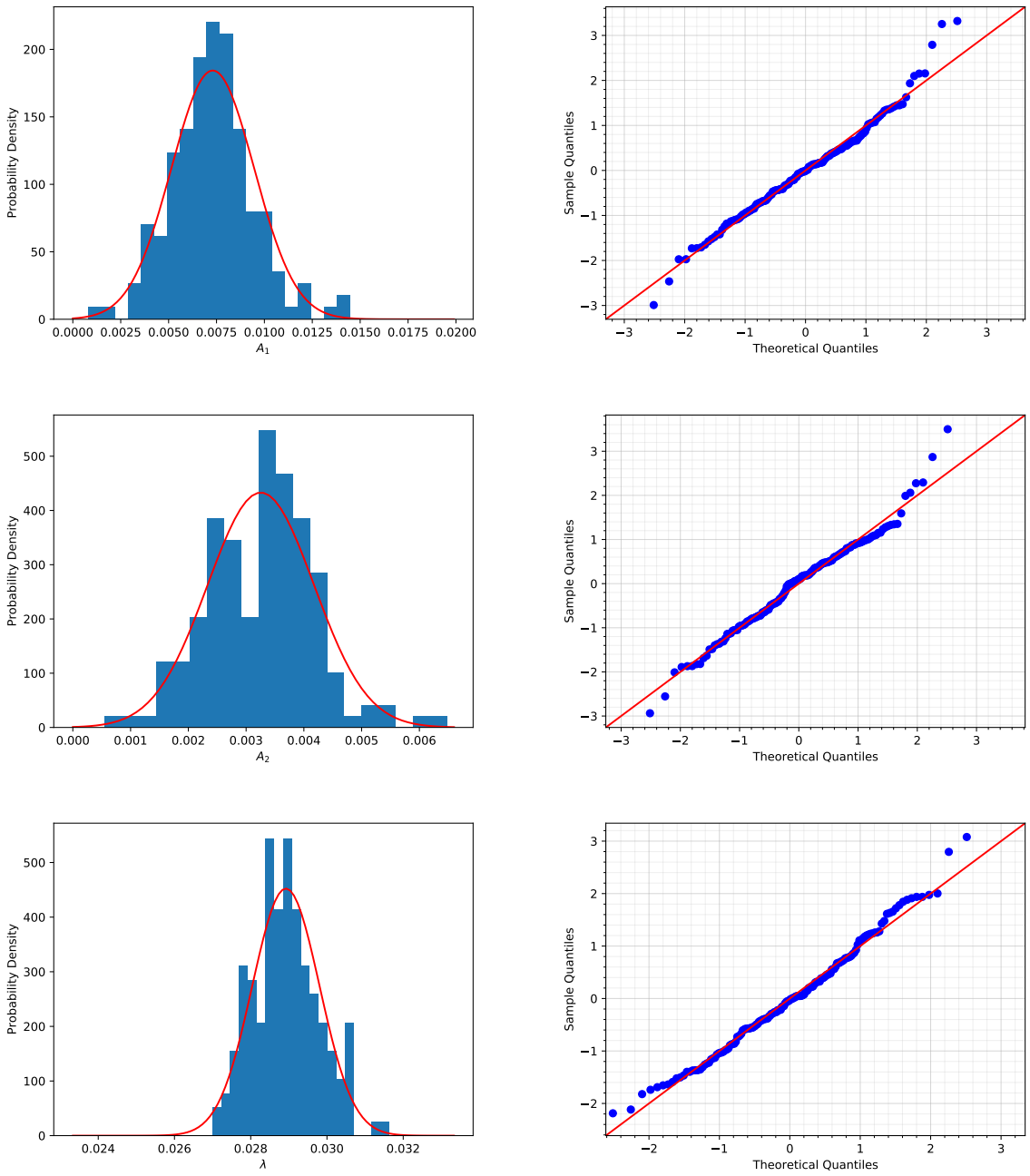

Figure 8: **Normalized model parameter values for hyperglycemic episodes** In the left column, the blue columns form the histogram for each normalized parameter value distributed into ten bins of equal width. The red curve denotes the normal distribution with mean and variance that matches the sample mean and variance of each corresponding parameter. The right column are Q-Q plots for each model parameter. The rows, from top to bottom, correspond to the parameters A_1, A_2, and λ. The units of the parameters are $[A_1] = [A_2] = \text{litre}/(\text{min} \times \text{mmol})$, and $[\lambda] = 1/\text{min}$.

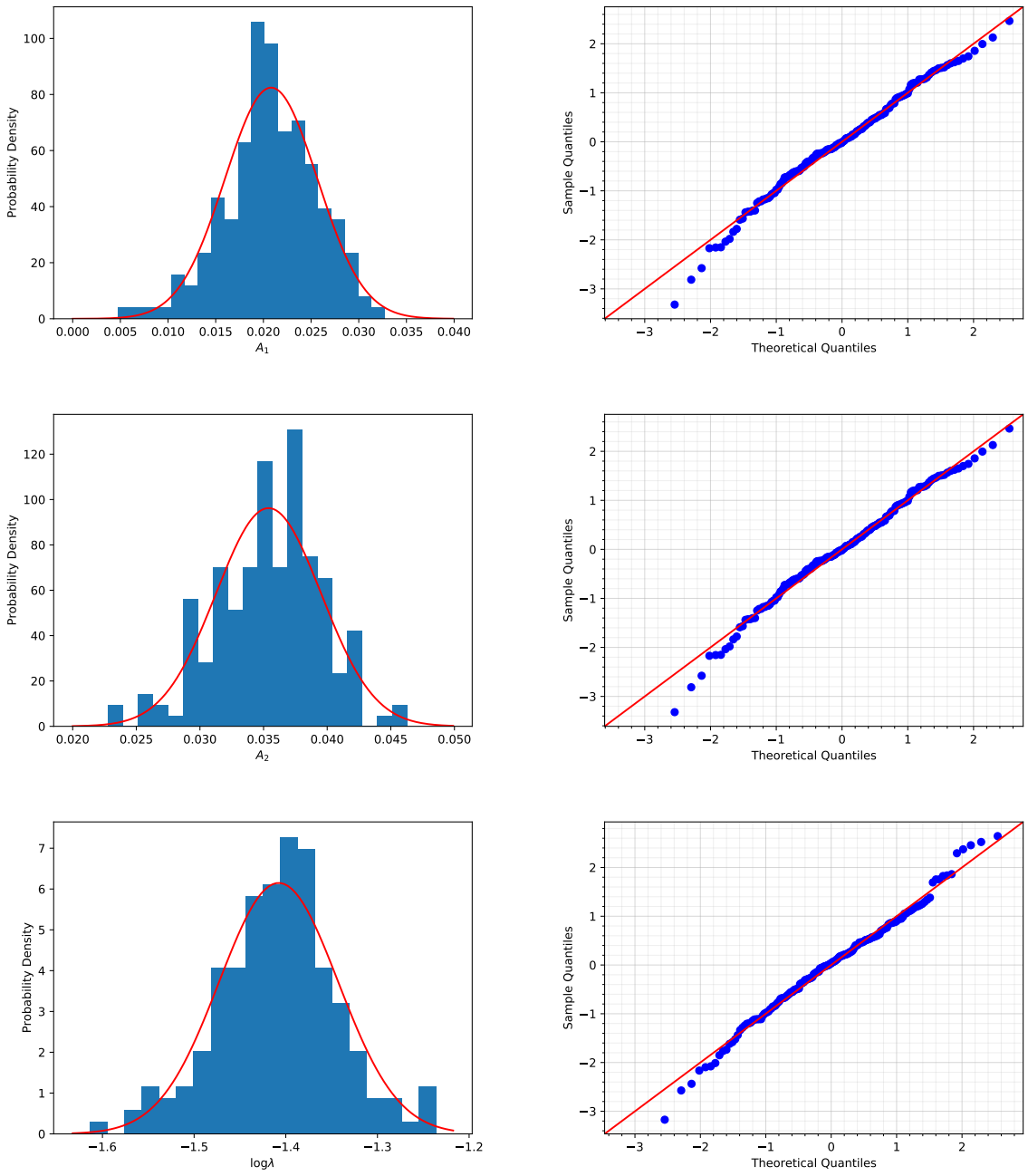

Figure 9: **Normalized model parameter values for hyperglycemic episodes** In the left column, the blue columns form the histogram for each normalized parameter value distributed into ten bins of equal width. The red curve denotes the normal distribution with mean and variance that matches the sample mean and variance of each corresponding parameter. The right column are Q-Q plots for each model parameter. The rows, from top to bottom, correspond to the parameters A_1, A_2, and $\log \lambda$. The units of the parameters are $[A_1] = [A_2] = \text{litre}/(\text{min} \times \text{mmol})$, and $[\log \lambda] = \log(1/\text{min})$.

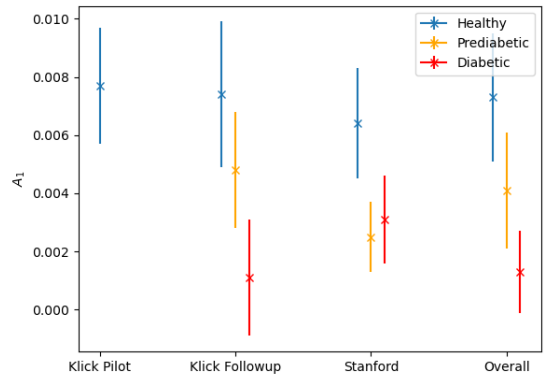

(a) A_1 Hyperglycemic

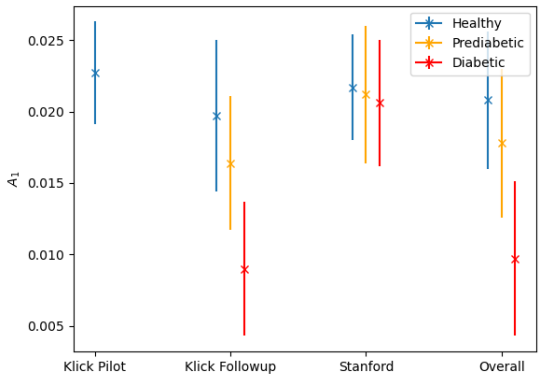

(b) A_1 Hypoglycemic

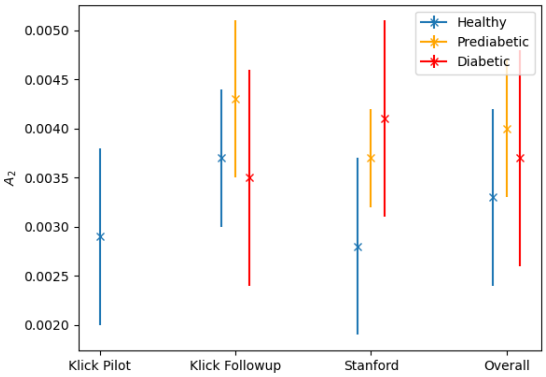

(c) A_2 Hyperglycemic

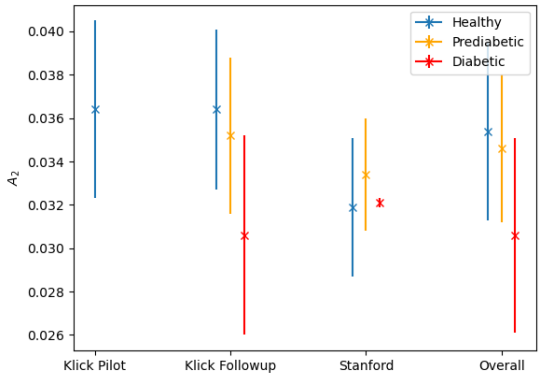

(d) A_2 Hypoglycemic

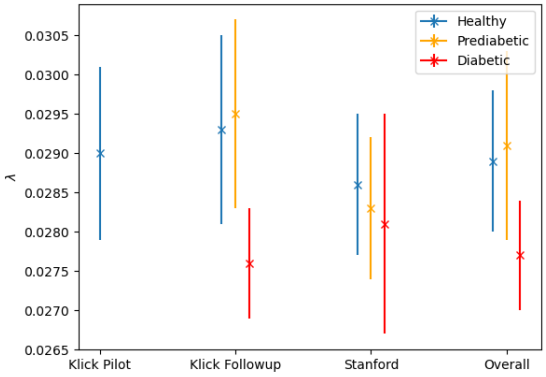

(e) λ Hyperglycemic

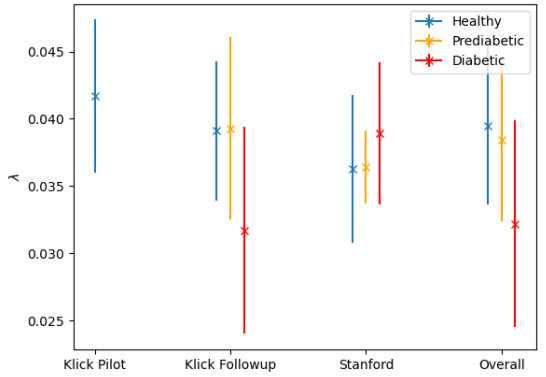

(f) λ Hypoglycemic

Figure 10: **Representation of Population Average and Standard Deviation for Parameters**. Parameters that were a result of the hyperglycemic system are shown on the left, and the parameters associated with the hypoglycemic system are shown on the right. Blue lines are for the healthy population, yellow is for the prediabetic population, and red is for the diabetic population.

The log-lambda distribution of the hypoglycemic system indicates a right-skewed distribution of lambda, with an increased amount of higher parameter values than in a normal distribution. As lambda is the inverse time scale of the memory kernal, the larger values represent decreased system memory. The physiological reason behind this can possibly be attributed to a few things. First, the production, secretion and elimination of glucagon varies from person to person, with the half life of glucagon ranging from 4 to 7 minutes [26]. Depending on the individual's response to low glucose levels, this may result in decreased system memory. Additionally, the controller, u, is an aggregation of control effects, which for the hypoglycemic system includes both glucagon and epinephrine. In times of stress epinephrine is released, resulting in almost instantaneous glucose increases [27]. This immediate increase occurs regardless of recent history of the system, which could result in the memory time scale being much smaller (and lambda subsequently becoming larger).

3.3 Application to Prediabetic/ Diabetic Individuals

Individuals selected for the study were considered diabetic using the guidelines provided by the American Diabetes Association, with A1c levels above 6.5%, FBG above 125 mg/dL and OGTT above 200 mg/dL. The resultant number of participants was $N = 52$, where $N = 4$ individuals were from the Stanford Study, $N = 9$ were from the first Klick Followup Study, and $N = 39$ were from the second Klick Followup Study.

Upon extracting the peaks and troughs of individual CGM data, the peaks and troughs of individuals were fitted to the model with a fitting error of 7.9027 ± 14.8001 ($E_{\max} = 93.9713$) and 0.0660 ± 0.2871 ($E_{\max} = 4.4833$) respectively, as defined in Eq 7.

Overall, diabetic individuals have selected peaks that deviate from the baseline for much longer and the deviations relative to baseline are much larger, which corresponds to the larger error E discussed above. For healthy individuals, most glucose deviations are approximately 1 mmol per litre above the baseline. For diabetic individuals, the glucose deviations can be 10 or more mmol above the baseline levels. This results in smaller A_1 values once the model has been fit to the data. Additionally, the error for the

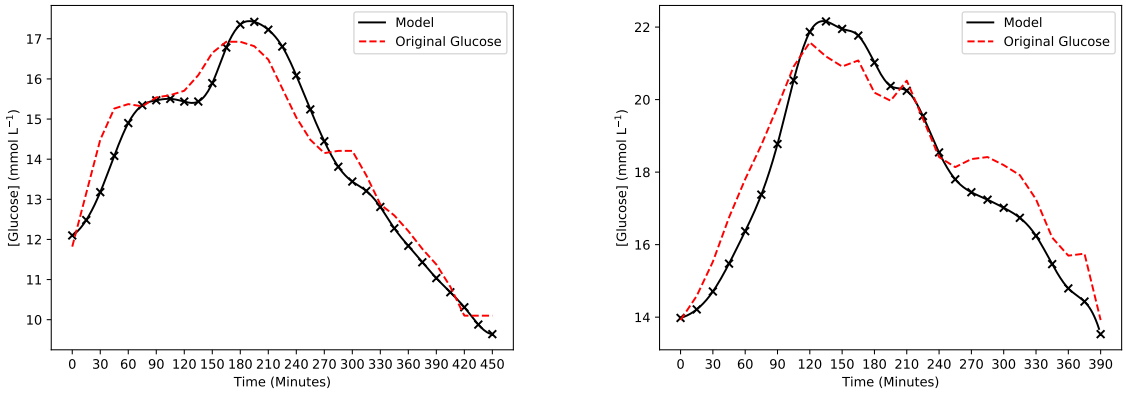

Figure 11: **Example results of the hyperglycemic model for diabetic individuals.** The original glucose data is represented by the red dashed lines. The set of black crosses is the model glucose output, and the black curve is the cubic spline interpolation of the model outputs.

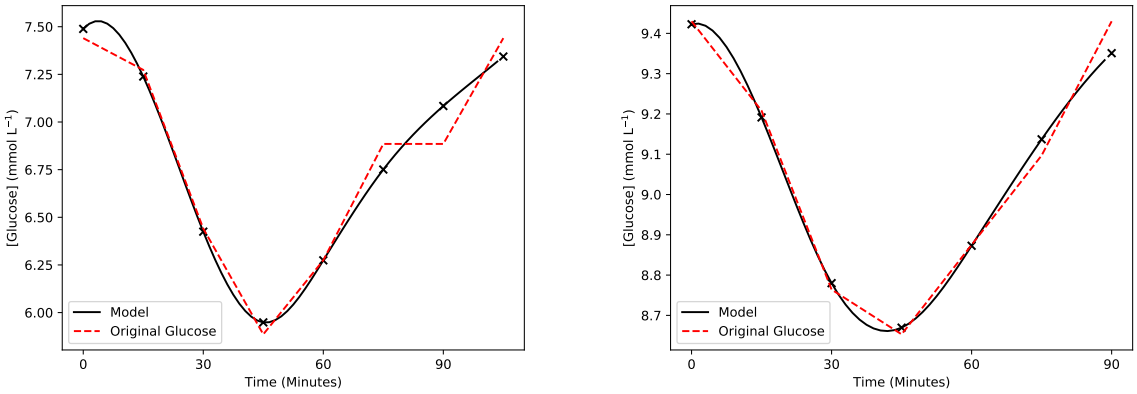

Figure 12: **Example results of the hypoglycemic model for diabetic individuals.** The original glucose data is represented by the red dashed lines. The set of black crosses is the model glucose output, and the black curve is the cubic spline interpolation of the model outputs.

hyperglycemic model for diabetic individuals is much greater than the error for healthy individuals, indicating a lack of control of the system.

Despite the baseline for diabetic individuals being larger than in healthy individuals, the negative deviations from baseline in these individuals are very similar to what is seen in healthy individuals on both length of time of the troughs and in the maximum relative deviation. The error is also very similar to what is seen in healthy individuals.

		Klick Follow-up	Stanford	Overall	p-value
Hyperglycemic	A_1	0.0011 ± 0.0020	0.0031 ± 0.0015	0.0013 ± 0.0021	$5.698e-05$
	A_2	0.0035 ± 0.0011	0.0041 ± 0.0010	0.0037 ± 0.0011	0.679
	λ	0.0276 ± 0.0007	0.0281 ± 0.0014	0.0277 ± 0.0007	$8.395e-05$
Hypoglycemic	A_1	0.0090 ± 0.0047	0.0206 ± 0.0044	0.0097 ± 0.0054	0.116
	A_2	0.0306 ± 0.0046	0.0321 ± 0.0002	0.0306 ± 0.0045	0.253
	λ	0.0317 ± 0.0077	0.0389 ± 0.0053	0.0322 ± 0.0077	0.115

Table 3: **Ranges of model parameters for diabetic individuals.** Model parameter ranges for hyperglycemic and hypoglycemic cases with their respectively p-values of the Shapiro-Wilk test for normality. The null-hypothesis H_0 states that the model parameters are normally distributed. The decision to reject or not reject H_0 is based on a critical p-value of 0.05.

Individuals selected for the study were considered prediabetic using the guidelines provided by the American Diabetes Association, where A1c levels are between 5.7% and 6.5%, FBG between 100 mg/dL and 125 mg/dL and OGTT between 140 mg/dL and below 200 mg/dL. For the studies in which HbA1c, OGTT, and FBG tests were performed, the individual was classified as prediabetic if their OGTT was between 7.8 mmol/litre and 11.1 mmol/litre, or if **both** their HbA1c and FBG levels were within prediabetic ranges. In the second Klick Followup study, only HbA1c measurements were taken (no OGTT), so they were classified exclusively using the threshold for HbA1c. The resultant number of participants was $N = 77$, where $N = 11$ individuals were from the Stanford Study, $N = 16$ were from the Klick Followup Study 1, and $N = 50$ were from the Klick Followup Study 2. Overall, prediabetic individuals had a high proportion of "healthy" glucose deviations in their CGM data (deviation from baseline approximately 1 mmol per litre), but had some larger deviations similar to those seen in the diabetic population (deviation from baseline approximately 4 mmol per litre). When the data was fit to the hyperglycemic and hypoglycemic model, the error was 1.3585 ± 2.6422 ($E_{\max} = 56.2137$) and 0.02043 ± 0.0759 ($E_{\max} = 1.4273$).

		Klick Follow-up	Stanford	Overall	p-value
Hyperglycemic	A_1	0.0048 ± 0.0020	0.0025 ± 0.0012	0.0041 ± 0.0020	0.629
	A_2	0.0043 ± 0.0008	0.0037 ± 0.0005	0.0040 ± 0.0007	0.687
	λ	0.0295 ± 0.0012	0.0283 ± 0.0009	0.0291 ± 0.0012	0.839
Hypoglycemic	A_1	0.0164 ± 0.0047	0.0212 ± 0.0048	0.0178 ± 0.0052	0.191
	A_2	0.0352 ± 0.0036	0.0334 ± 0.0026	0.0346 ± 0.0034	0.902
	λ	0.0393 ± 0.0068	0.0364 ± 0.0027	0.0384 ± 0.0060	0.191

Table 4: **Ranges of model parameters for prediabetic individuals.** Model parameter ranges for hyperglycemic and hypoglycemic cases with their respective p-values of the Shapiro-Wilk test for normality. The null-hypothesis H_0 states that the model parameters are normally distributed. The decision to reject or not reject H_0 is based on a critical p-value of 0.05.

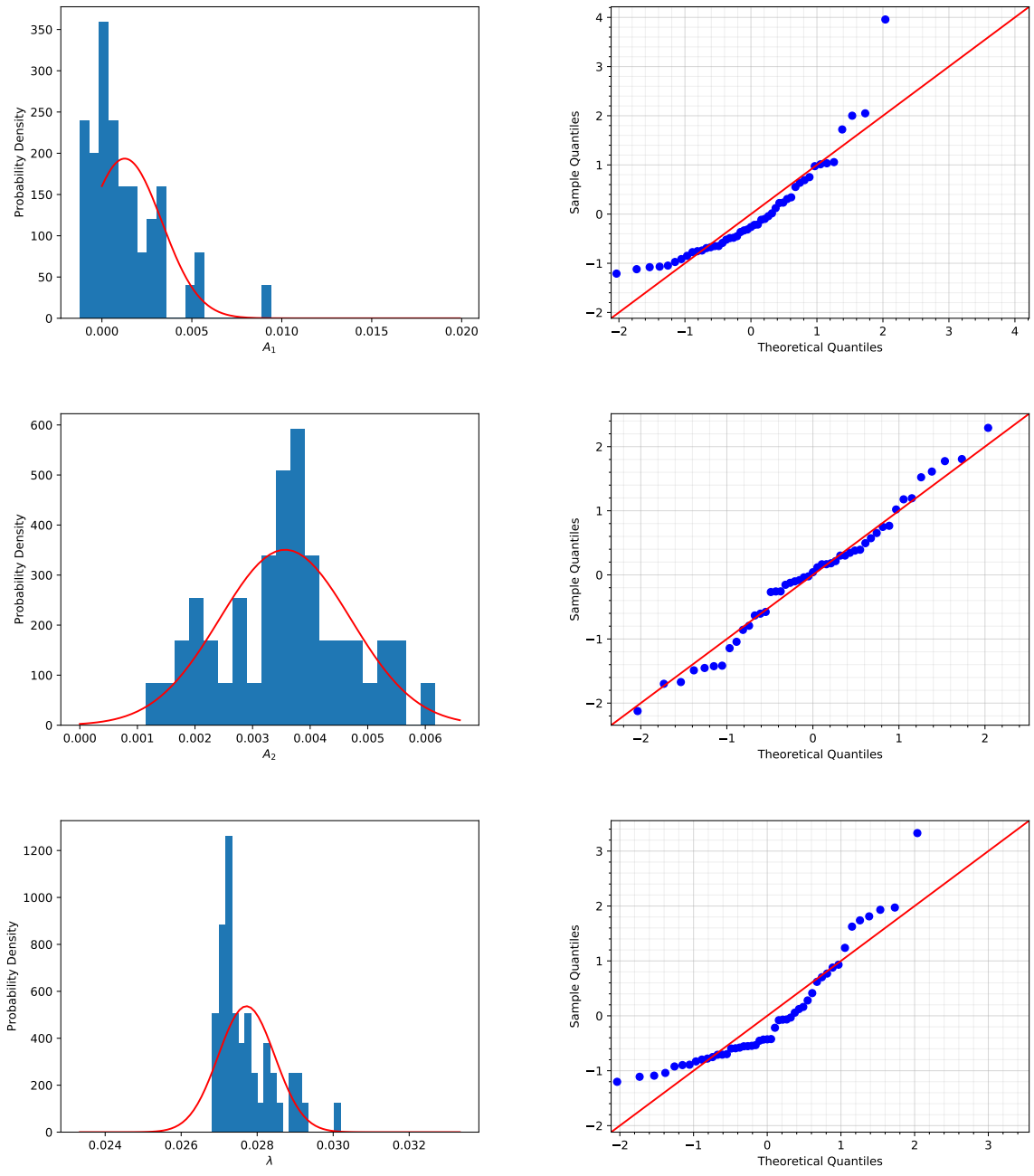

Figure 13: **Normalized model parameter values for hyperglycemic cases for diabetic individuals.** In the left column, the blue columns form the histogram for each normalized parameter value distributed into ten bins of equal width. The red curve denotes the normal distribution with mean and variance that matches the sample mean and variance of each corresponding parameter. The right column are Q-Q plots for each model parameter. The rows, from top to bottom, correspond to the parameters A_1, A_2, and λ. The units of the parameters are $[A_1] = [A_2] = \text{litre}/(\text{min} \times \text{mmol})$, and $[\lambda] = 1/\text{min}$.

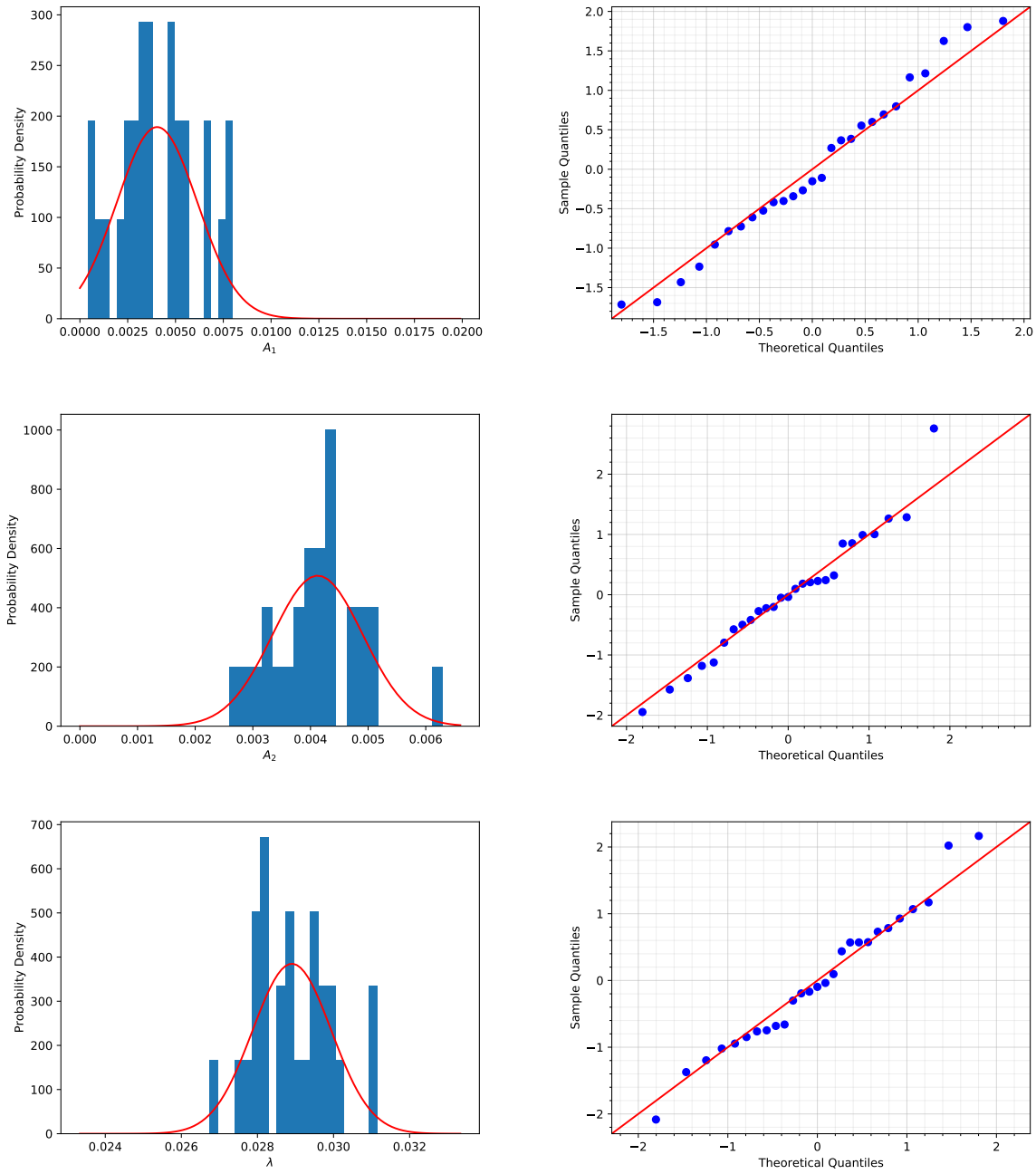

Figure 14: **Normalized model parameter values for hyperglycemic cases for prediabetic individuals.** In the left column, the blue columns form the histogram for each normalized parameter value distributed into ten bins of equal width. The red curve denotes the normal distribution with mean and variance that matches the sample mean and variance of each corresponding parameter. The right column are Q-Q plots for each model parameter. The rows, from top to bottom, correspond to the parameters A_1, A_2, and λ. The units of the parameters are $[A_1] = [A_2] = \text{litre}/(\text{min} \times \text{mmol})$, and $[\lambda] = 1/\text{min}$.

4 Biomarkers

One of the objectives of this research was to use the parameters that were obtained through model fitting to the CGM data to predict the diabetic status of individuals with type 2 diabetes or prediabetes. This notion stems from the idea of biomarkers. A biomarker is a defined, measureable characteristic that indicates a normal biological process, a disease process, or a response to exposure or intervention. Some common example of biomarkers are blood pressure and pulse. These metrics can be used to distinguish healthy individuals from individuals in a disease state.

Although the hypoglycemic system may be impacted by type 2 diabetes, there is substantially more evidence supporting the difference in the glucose-insulin (hyperglycemic) system between healthy individuals and individuals with type 2 diabetes. As such, the parameters analyzed in this section will come exclusively from the hyperglycemic peak fitting.

4.1 Initial Type 2 Diabetes Biomarker

The first attempt at a biomarker from this model came from the paper published by van Veen et al. in 2020. Five glucose peaks of similar length were averaged together to form a single representative peak. Gradient descent was run on this single peak, and the resulting parameters A_1 and A_2 were scaled by the standard deviation of the raw CGM time series divided by the maximum value of the controller for that peak. In the paper, it was predicted that the scaled A_1 would decrease and the scaled A_2 would increase as individuals become more diabetic. This prediction was due to the shapes of the peaks themselves, as longer, more sustained glucose deviations in healthy individuals were characterized by low A_1 and high A_2. It was concluded that diabetic individual peaks would be longer, with a more gradual decline than individuals with a healthy glucose homeostasis [20].

A similar attempt at a biomarker was made with the current data and method. However, some modifications had to be made, as the current method involves fitting all 80-150 selected peaks of different lengths. Rather than taking the parameter output from a single representative peak (as was done by van Veen [20]), the A_1 and A_2 parameter values obtained from performing gradient descent on all 80-150 peaks were averaged. A figure depicting only the healthy and diabetic averaged A_1 and A_2 parameter values, and the healthy, prediabetic, and diabetic averaged A_1 and A_2 parameter values can be seen in Figure 15. The class of the individual was determined using the same criteria as in Section 3.

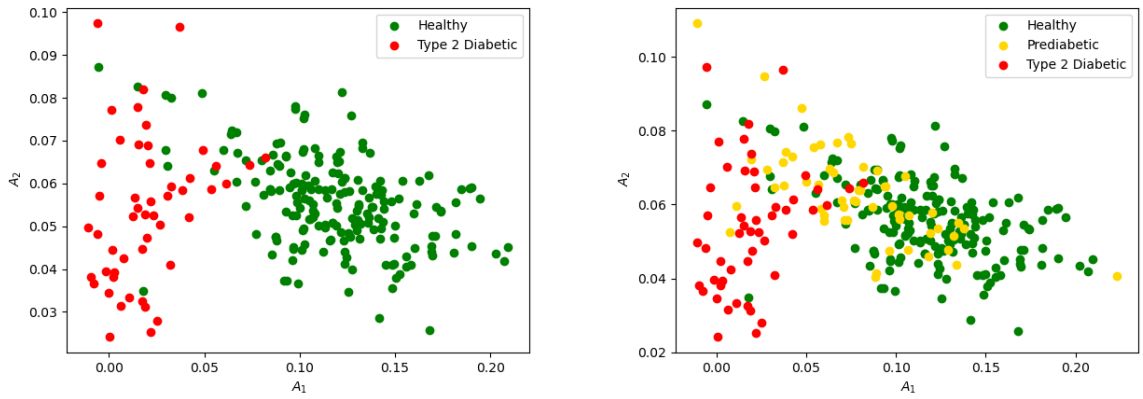

Figure 15: **Average A_1 & A_2, Comparing Diagnostics.** The image on the left depicts the average A_1 and A_2 calculated values for each healthy and diabetic individual. Red dots denote diabetic individuals and green dots denote healthy individuals. The image on the right depicts the average A_1 and A_2 calculated values for each healthy, diabetic, and prediabetic individual. Red dots denote diabetic individuals, yellow dots denote prediabetic individuals and green dots denote healthy individuals.

To get a more comprehensive comparison between this metric and the one calculated by van Veen et al., the values will be scaled by the standard deviation of the raw CGM divided by the average maximum value of the controller for each individual. This can be seen in Figure 16.

Other metrics were also analyzed for validity. The range of the A_1 and A_2 values was calculated and plotted against each other. These values were also scaled using the same factor described above. The results can be seen in Figure 17.

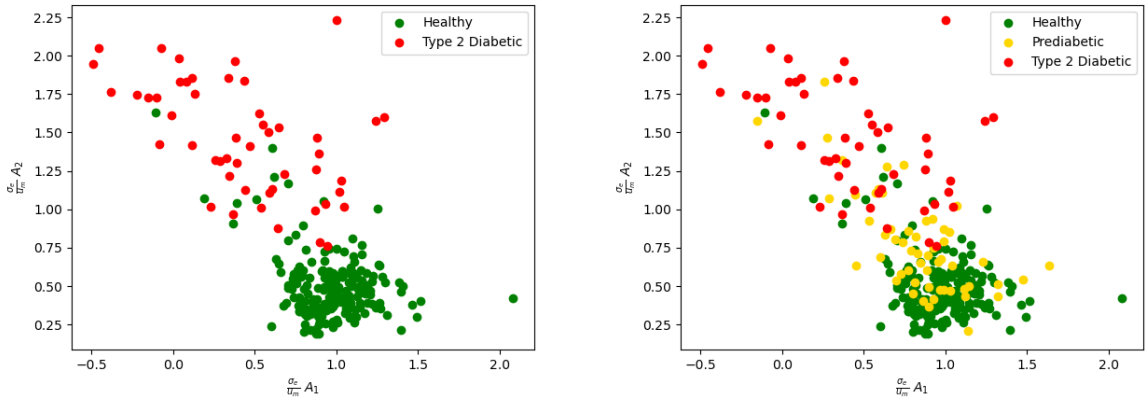

Figure 16: **Scaled Average A_1 & A_2, Comparing Diagnostics.** The image on the left depicts the average A_1 and A_2 calculated values for each healthy and diabetic individual, scaled by the standard deviation of the entire CGM time series, σ_e, divided by the average maximum value of the controller, u_m. Red dots denote diabetic individuals and green dots denote healthy individuals. The image on the right depicts the average A_1 and A_2 calculated values for each healthy, diabetic, and prediabetic individual, scaled by the standard deviation of the entire CGM time series, σ_e, divided by the average maximum value of the controller, u_m. Red dots denote diabetic individuals, yellow dots denote prediabetic individuals and green dots denote healthy individuals.

Finally, the standard deviation of A_1 and A_2 values was used. These values were also scaled using the factor above, and can be seen in Figure 18.

4.1.1 Separation Based on Gender

There is currently no distinction between males and females for the thresholds of the current diagnostic methods. However, males and females differ physiologically in their glucose control. Before menopause, women have high concentrations of estrogens in their bloodstream. Concentrations can be 15-350 pg/mL for estradiol and 17-200 pg/mL for estrone, depending on their point in their menstruation cycle. On the other hand, men have 10-40 pg/mL of estradiol and 10-60 pg/mL of estrone at any point (CITE). This is significant for glucose homeostasis, as estrogen has direct effects on insulin and energy metabolism. Studies have shown that estrogen increases sensitivity of insulin to insulin-sensitive tissues, has effects on β-cells in the pancrease to regulate insulin release, and also has effects in the liver and adipose fat

tissue to regulate glucose release into the bloodstream [28].

Due to the recorded difference in glucose homeostasis between the genders, the analysis performed to obtain a biomarker of diabetic status will also be performed on each gender separately. For females, scaled and unscaled average parameter values of A_1 and A_2 can be seen in Figure 19. Parameter range results for females can be seen in Figure 20, and parameter standard deviation results for females can be seen in Figure 21. For males, average parameter results are seen in Figure 22, parameter range results can be seen in Figure 23, and parameter standard deviation results can be seen in Figure 24.

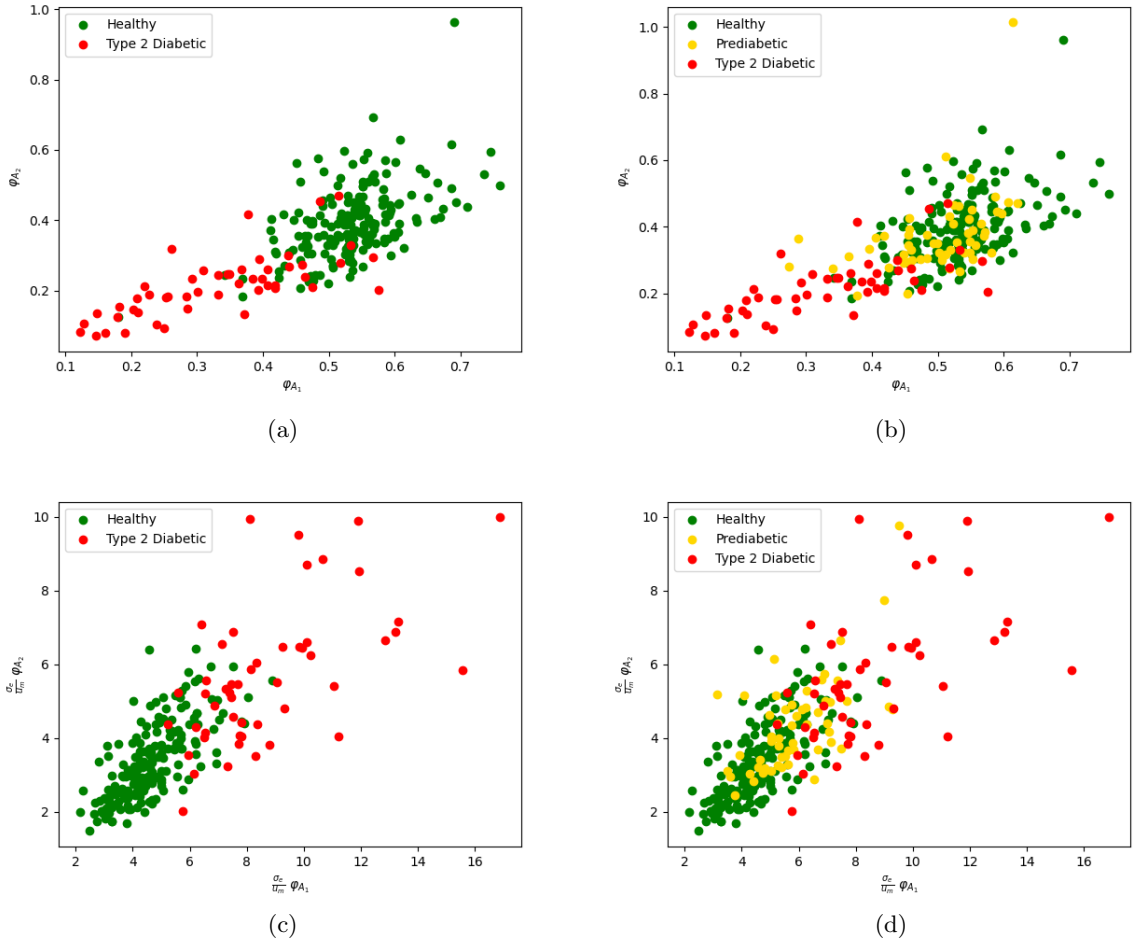

Figure 17: **Range A_1 & A_2, Comparing Diagnostics.** The range of parameter values (difference between the maximum parameter value and the minimum parameter value) is plotted for A_1 and A_2 for each individual, shown as φ_{A_1} and φ_{A_2} respectively. Healthy and diabetic individuals are shown in green and red respectively. Prediabetic individuals are shown in yellow in (b) and (d). (a) and (b) are the unscaled range, and (c) and (d) are the range scaled by the standard deviation of the entire CGM time series divided by the average maximum value of the controller, u.

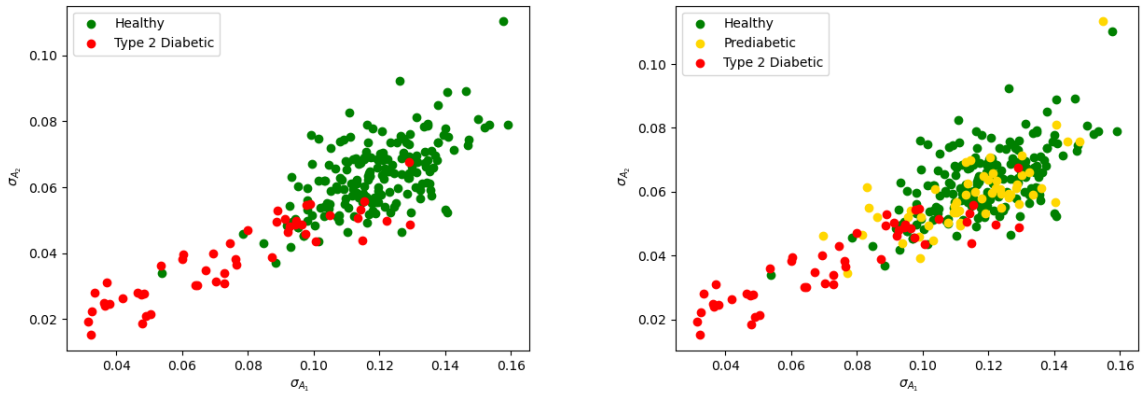

(a) (b)

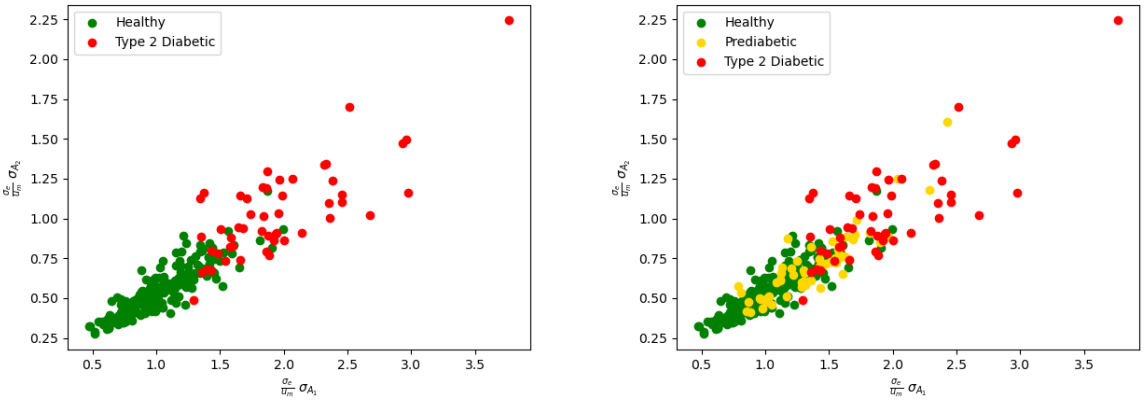

(c) (d)

Figure 18: **Standard Deviation A_1 & A_2, Comparing Diagnostics.** The standard deviation of parameter values is plotted for A_1 and A_2 for each individual, shown as σ_{A_1} and σ_{A_2} respectively. Healthy and diabetic individuals are shown in green and red respectively. Prediabetic individuals are shown in yellow in (b) and (d). (a) and (b) are the unscaled standard deviation, and (c) and (d) are the standard deviation of the parameters A_1 and A_2, scaled by the standard deviation of the entire CGM time series divided by the average maximum value of the controller, u.

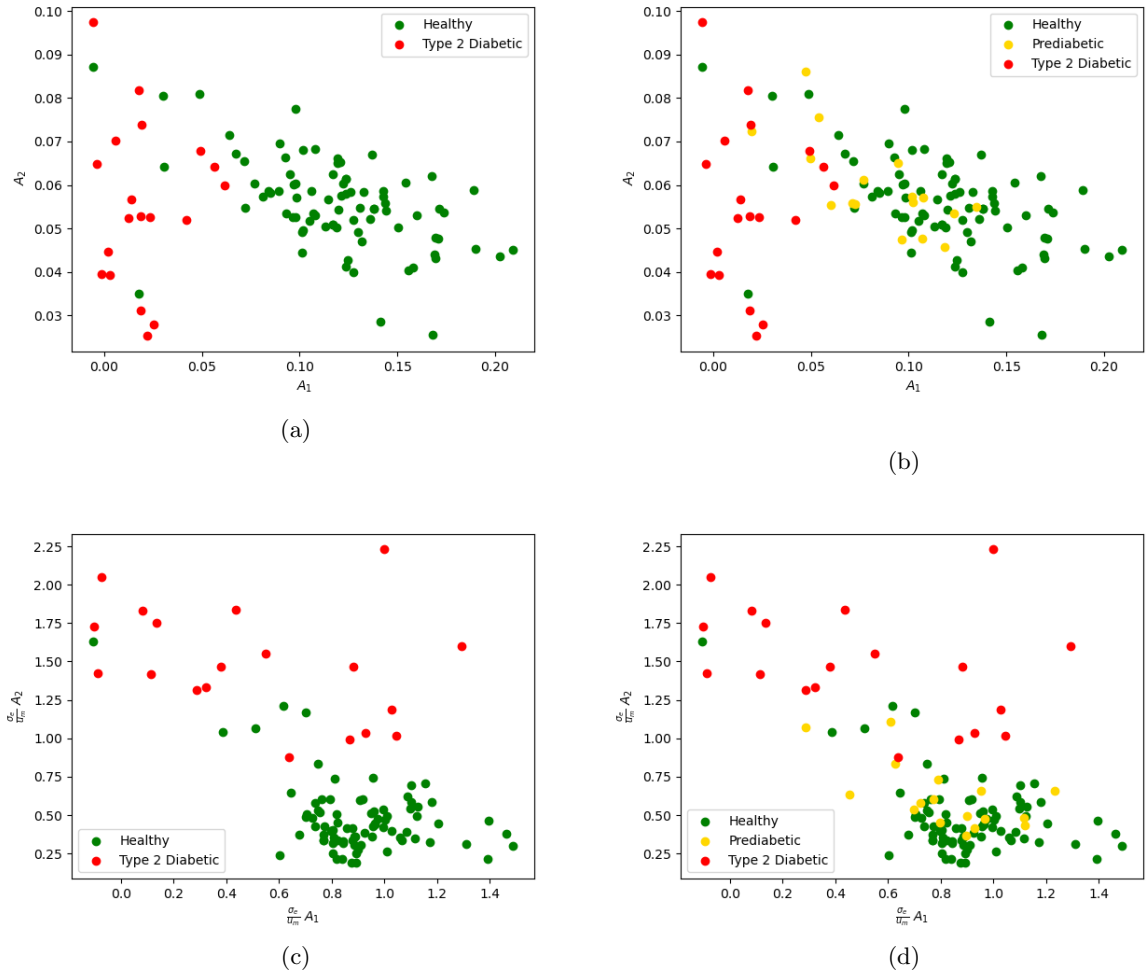

Figure 19: **Average A_1 & A_2, Comparing Diagnostics, Females.** The averaged parameter values are plotted for A_1 and A_2 for each individual. Healthy and diabetic individuals are shown in green and red respectively. Prediabetic individuals are shown in yellow in (b) and (d). (a) and (b) are the unscaled average, and (c) and (d) are the average of the parameters A_1 and A_2, scaled by the standard deviation of the entire CGM time series, σ_e, divided by the average maximum value of the controller, u_m.

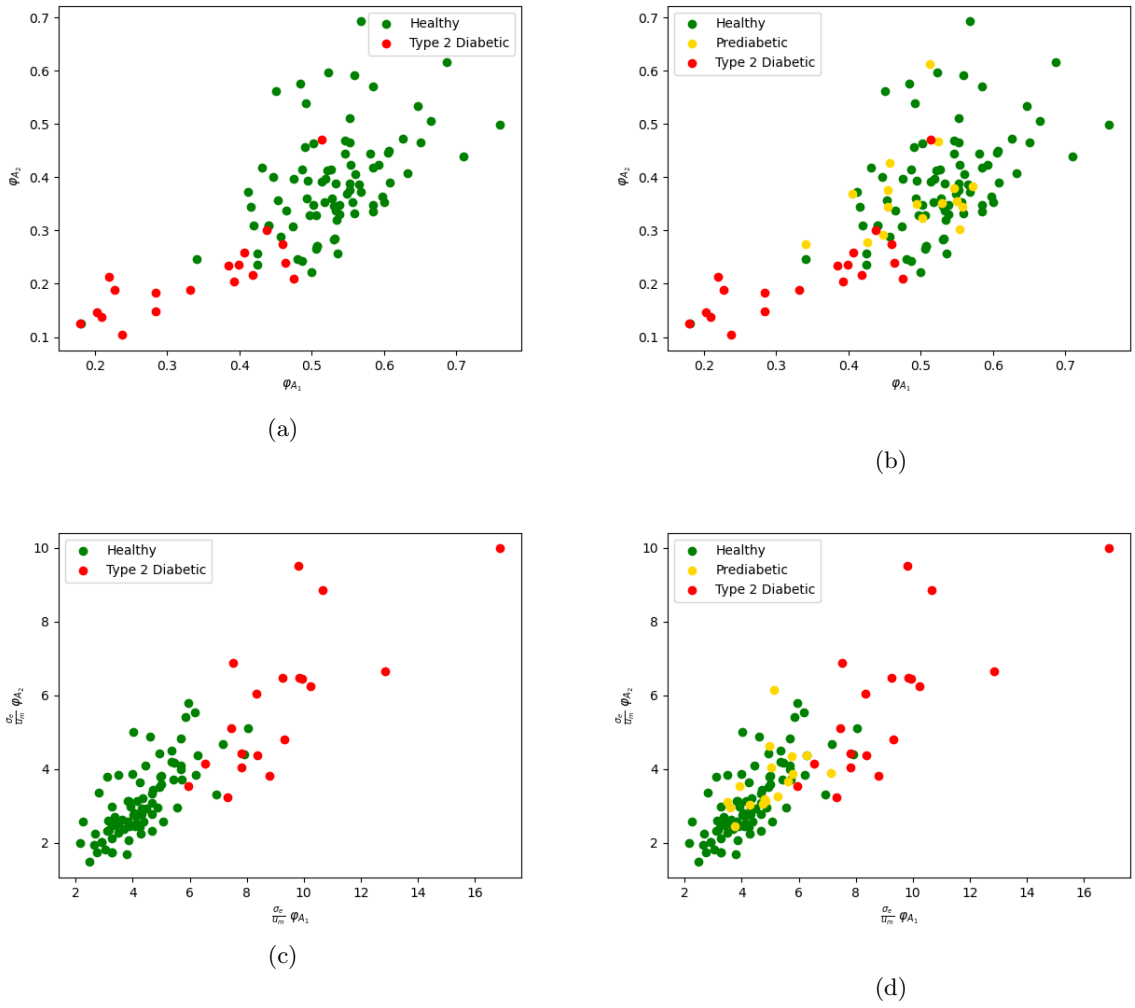

Figure 20: **Range A_1 & A_2, Comparing Diagnostics, Females.** The range of parameter values is plotted for A_1 and A_2 for each individual, shown as φ_{A_1} and φ_{A_2}. Healthy and diabetic individuals are shown in green and red respectively. Prediabetic individuals are shown in yellow in (b) and (d). (a) and (b) are the unscaled range, and (c) and (d) are the range scaled by the standard deviation of the entire CGM time series, σ_e, divided by the average maximum value of the controller, u_m.

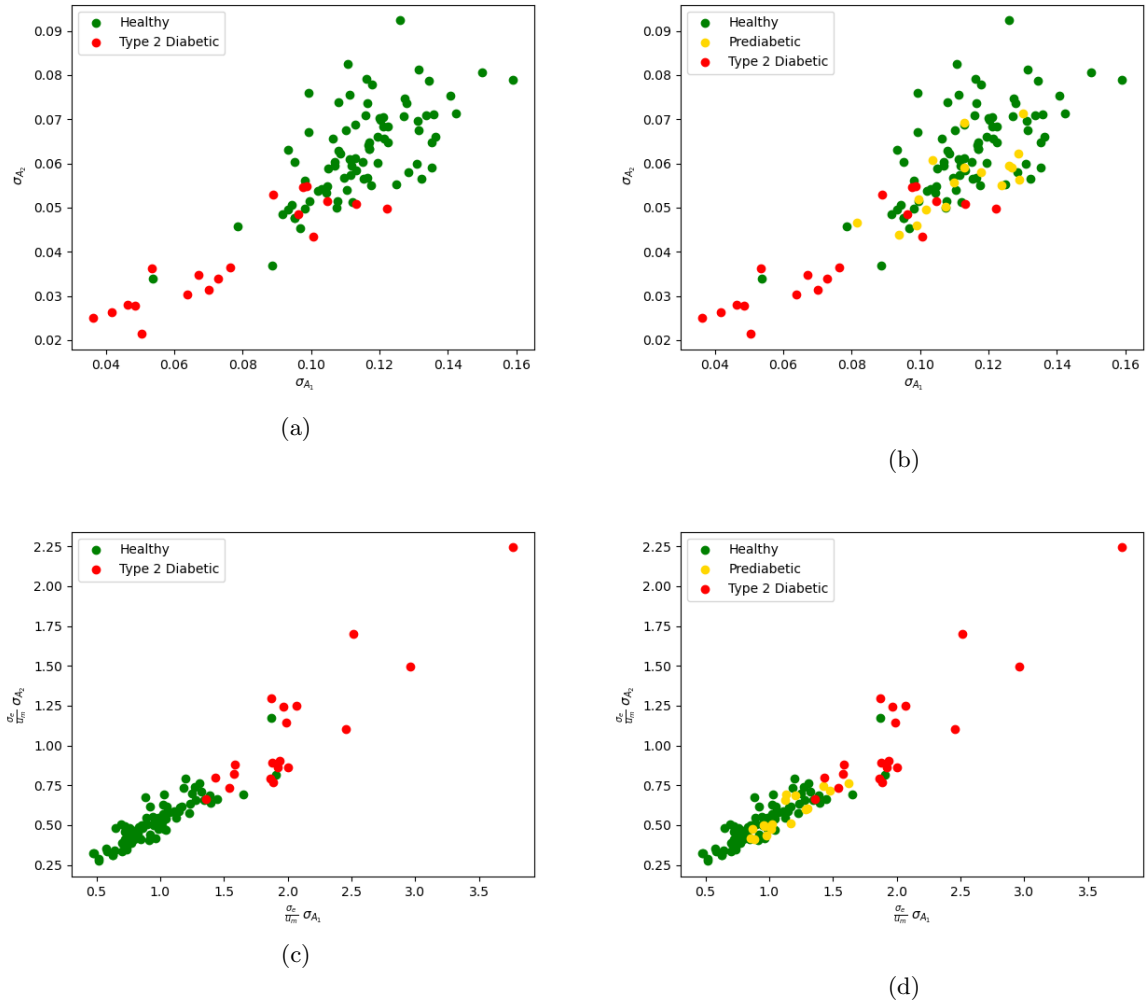

Figure 21: **Standard Deviation A_1 & A_2, Comparing Diagnostics, Females.** The standard deviation of parameter values is plotted for A_1 and A_2 for each individual, shown as σ_{A_1} and σ_{A_2}. Healthy and diabetic individuals are shown in green and red respectively. Prediabetic individuals are shown in yellow in (b) and (d). (a) and (b) are the unscaled standard deviation, and (c) and (d) are the standard deviation of the parameters A_1 and A_2, scaled by the standard deviation of the entire CGM time series, σ_e, divided by the average maximum value of the controller, u_m.

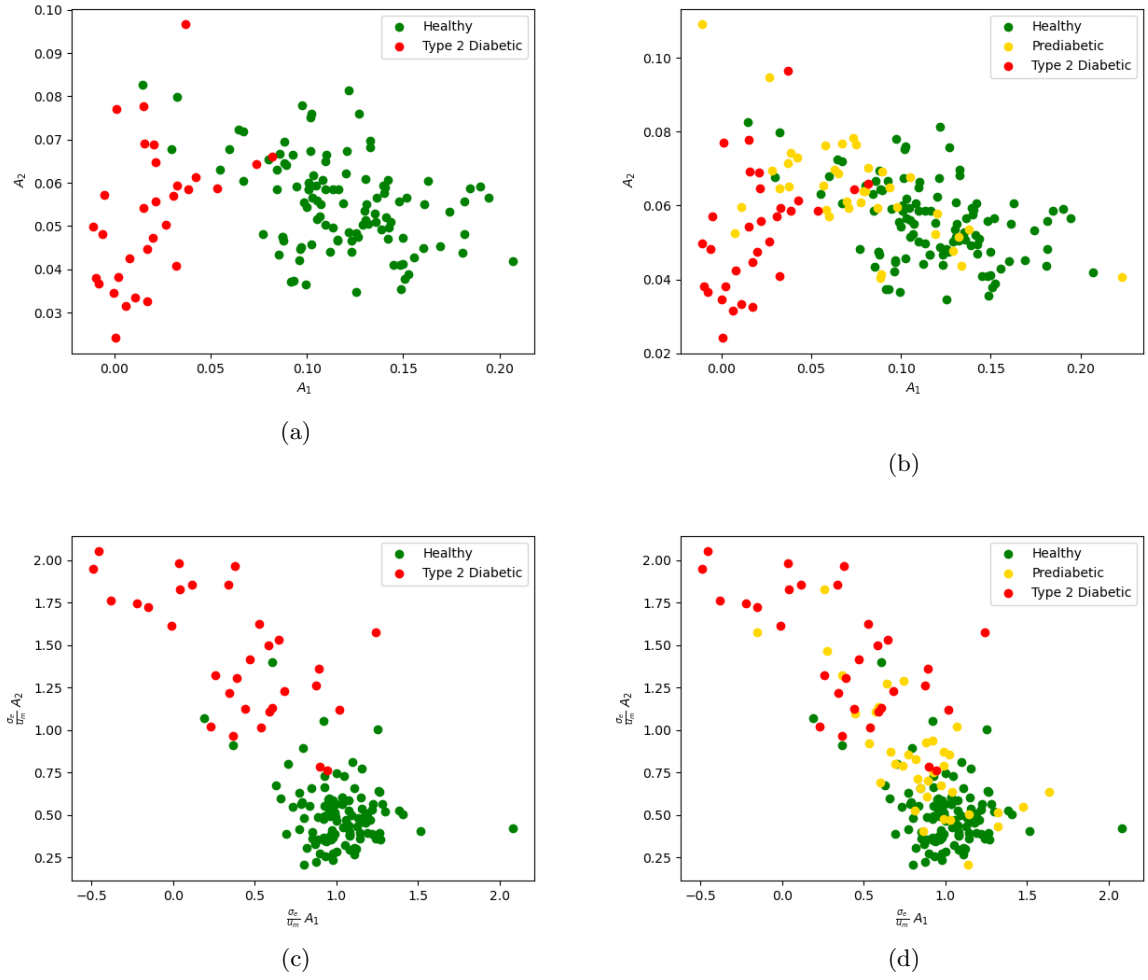

Figure 22: **Average A_1 & A_2, Comparing Diagnostics, Males.** The averaged parameter values are plotted for A_1 and A_2 for each individual. Healthy and diabetic individuals are shown in green and red respectively. Prediabetic individuals are shown in yellow in (b) and (d). (a) and (b) are the unscaled average, and (c) and (d) are the average of the parameters A_1 and A_2, scaled by the standard deviation of the entire CGM time series, σ_e, divided by the average maximum value of the controller, u_m.

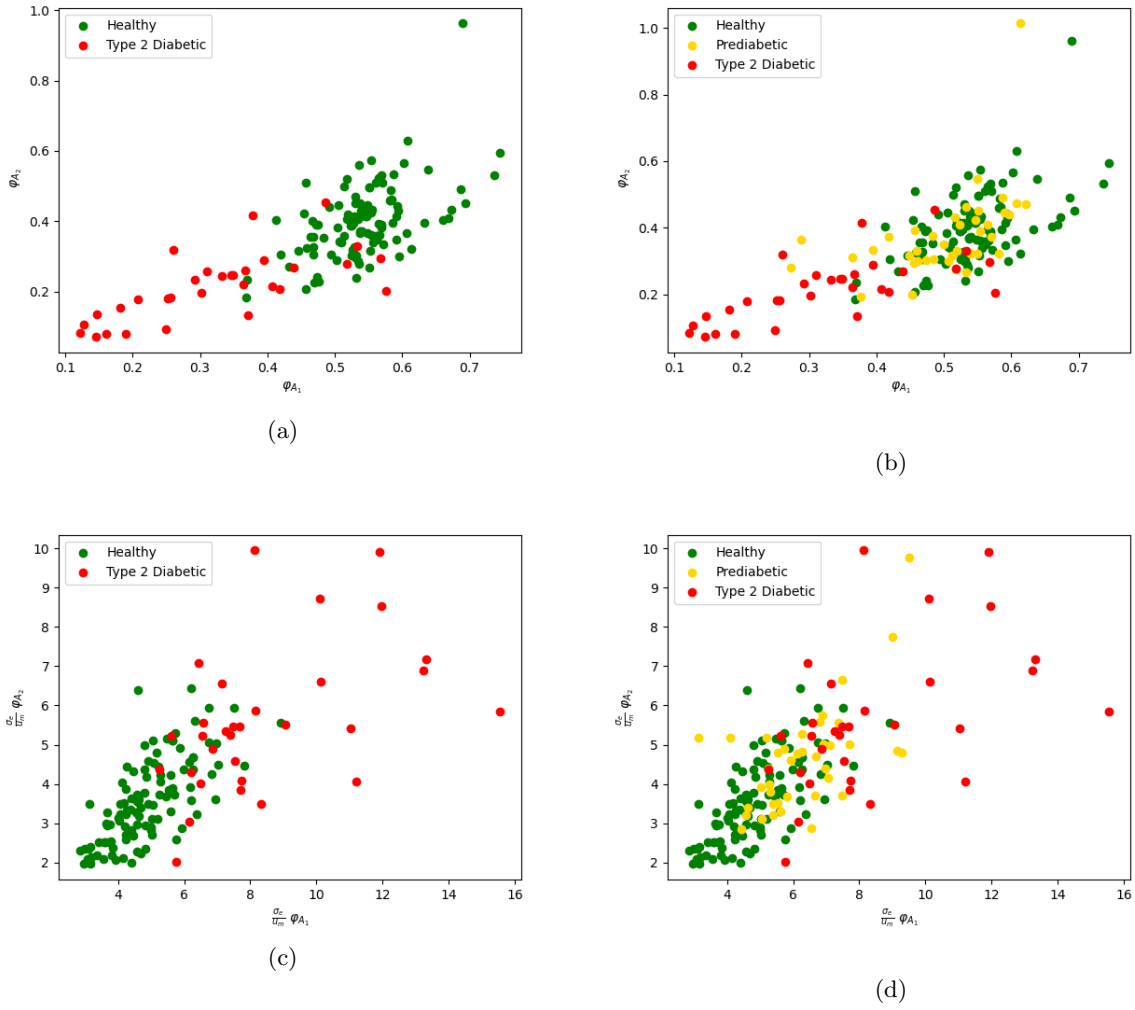

Figure 23: **Range A_1 & A_2, Comparing Diagnostics, Males.** The range of parameter values is plotted for A_1 and A_2 for each individual, shown as φ_{A_1} and φ_{A_2}. Healthy and diabetic individuals are shown in green and red respectively. Prediabetic individuals are shown in yellow in (b) and (d). (a) and (b) are the unscaled range, and (c) and (d) are the range scaled by the standard deviation of the entire CGM time series, σ_e, divided by the average maximum value of the controller, u_m.

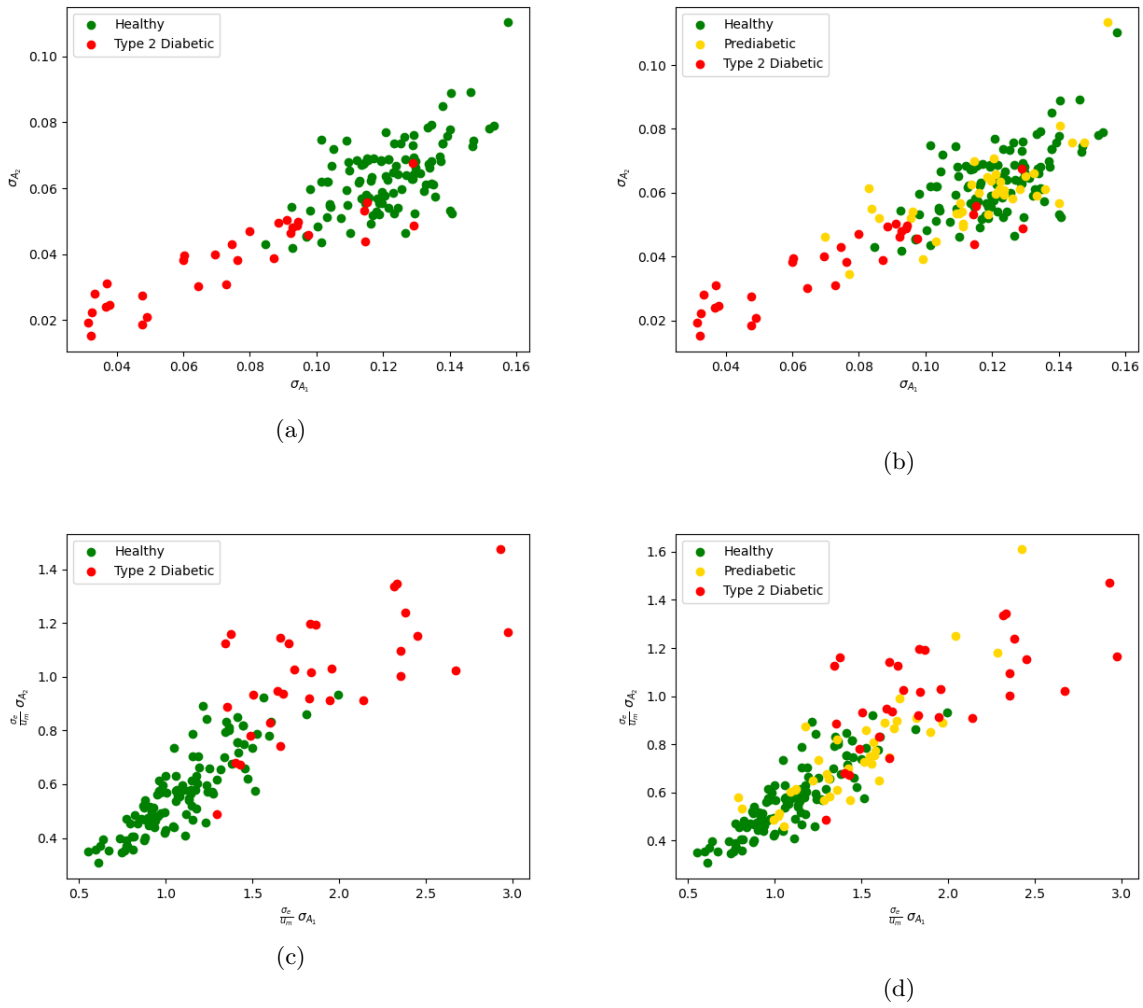

Figure 24: **Standard Deviation A_1 & A_2, Comparing Diagnostics, Males.** The standard deviation of parameter values is plotted for A_1 and A_2 for each individual, shown as σ_{A_1} and σ_{A_2}. Healthy and diabetic individuals are shown in green and red respectively. Prediabetic individuals are shown in yellow in (b) and (d). (a) and (b) are the unscaled standard deviation, and (c) and (d) are the standard deviation of the parameters A_1 and A_2, scaled by the standard deviation of the entire CGM time series, σ_e, divided by the average maximum value of the controller, u_m.

By looking at the scaled and unscaled parameter distributions, there is a fairly clear progression of diabetic status. Starting with the cases in which gender was not separated for unscaled A_1 and A_2 (Figure 15) results dictated that A_1 values for healthy individuals were moderate-high comparatively to the A_1 values of all the participants. Average A_1 values were low for diabetic individuals compared to the A_1 values of all the participants. For prediabetic individuals, parameter results were between the average values for diabetic and healthy individuals, with moderate average A_1 values and high A_2 values compared to the rest of the data.

Looking at the case in which the average A_1 and A_2 values are scaled by the standard deviation of the glucose data and the maximum value of the controller, u, healthy individuals have scaled A_1 that are high, and low scaled A_2 values. For diabetic individuals, scaled A_1 is low and scaled A_2 is high. Prediabetic individuals fall between healthy and diabetic individuals, with moderate scaled A_1 and A_2 values.

We can compare this to the hypothesis proposed in van Veen et al. (2020). The article hypothesizes that the scaled average parameter values would decrease for A_1 and increase for A_2 as an individual becomes more diabetic, or their glucose homeostasis becomes less effective. Although this hypothesis is correct, particularly for diabetic individuals, it breaks down slightly when applied to prediabetic individuals. There is a slight shift of prediabetic individuals towards the upper left of the plot, however, the progression of healthy to T2D status is not as clear as indicated in the paper, with many prediabetic individuals overlapping heavily with healthy individuals. Thus, it becomes necessary to evaluate other metrics summarizing parameter results to determine if a more accurate predictor of glucose homeostasis effectiveness can be obtained.

The range (difference between the maximum value and minimum value) of parameter values A_1 and A_2 and the standard deviation of parameter values A_1 and A_2 were also evaluated, seen in 17 and 18. For the unscaled range and standard deviation of parameter values, both the metrics for A_1 and A_2 decreased as an individual became diabetic. For the scaled metrics, healthy individuals had low scaled

metrics for A_1 and A_2, and diabetic individuals had high scaled metrics for both the range and the standard deviation of A_1 and A_2. In the scaled and unscaled range and standard deviation, the prediabetic population was much more centralized to be between the diabetic and healthy population metrics than what was seen in the average parameter values in Figure 15 and 16.

The clearest separation of individuals is seen when the scaled standard deviation of the A_1 parameter is plotted against the scaled standard deviation of the A_2 parameter, in both the cases in which results were analyzed independently of gender and by separating based on gender. The two values have a strong positive linear relationship, with a linear correlation coefficient of 0.927 and a slope of 0.5 for the case of no gender separation.

Looking at the parameter results after gender separation, there is not much difference between males and females. Diabetic and prediabetic individuals appear at roughly the same coordinates for both males and females, and healthy individuals are all within the same range of values. It can be concluded that gender does not play much of an effect in the initial parameter analysis, however gender will continue to be separated for subsequent analysis in the event that more accurate results are yielded.

4.1.2 Single Value Homeostasis Biomarker

One of the objectives of this research is to evaluate an individual's glucose homeostasis. The simplest way to do this with the available results of model fitting is to create a single value biomarker that indicates glucose homeostasis effectiveness. To construct the biomarker, the sum of the scaled standard deviation of the A_1 parameter and two times the scaled standard deviation of the A_2 parameter will be taken. For a comprehensive metric of an individuals glucose homeostasis, this sum will then be multiplied by the individual's average glucose level. The full calculation of the homeostasis Biomarker is calculated as follows:

$$\text{Biomarker} = \frac{e_{avg}\sigma_e}{u_m} * (\sigma_{A_1} + 2 * \sigma_{A_2}) \tag{8}$$

Where e_{avg} is the average glucose value, σ_e is the standard deviation of the glucose, u_m is the average maximum value of the controller, σ_{A_1} is the A_1 parameter standard deviation, and σ_{A_2} is the A_2 parameter standard deviation. The smaller this biomarker is, the more effective the individual's homeostasis is. If the biomarker is large, it would indicate a dysfunctional glucose homeostasis. This biomarker will be in the same units as the blood glucose measurements, in this instance, mmol/L.

The calculated biomarker for healthy and diabetic individuals can be seen in Figure 25. Prediabetic individuals are added in Figure 26.

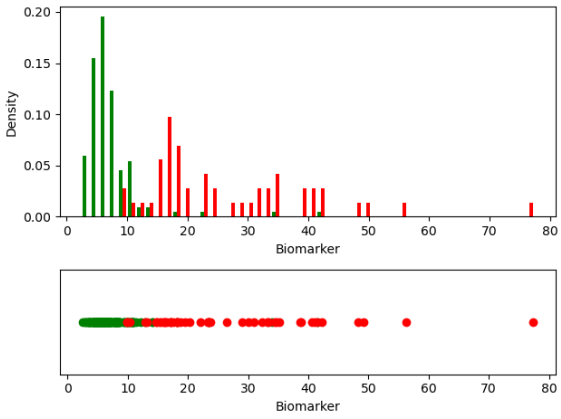

(a) Both Genders

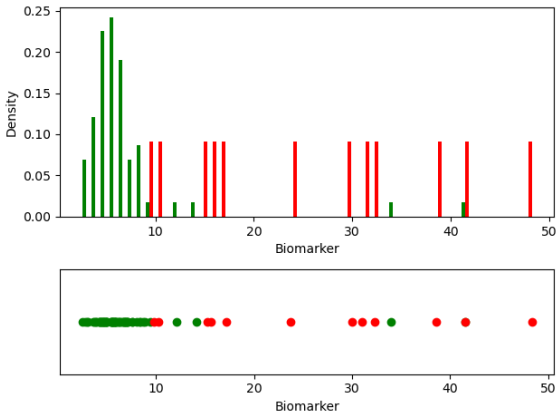

(b) Female

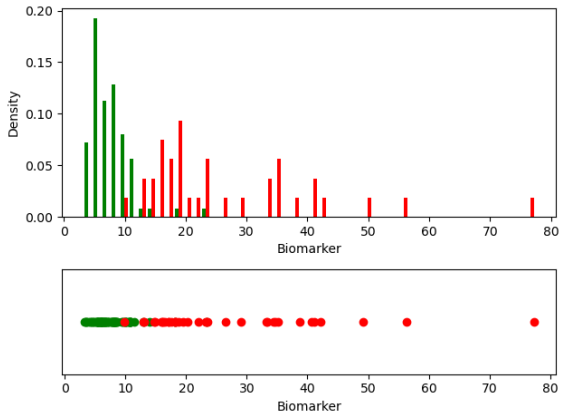

(c) Male

Figure 25: **Single Value Biomarker for Healthy and Type 2 Diabetic Individuals.** Biomarker is plotted for (a) both genders, (b) females only, and (c) males only. In each subfigure, the x-axis depicts the biomarker value, the y-axis in the histogram represents the histogram density. Red depicts diabetic individuals, green depicts healthy individuals.

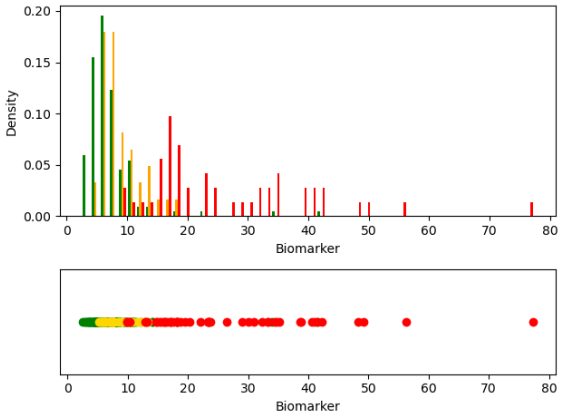

(a) Both Genders

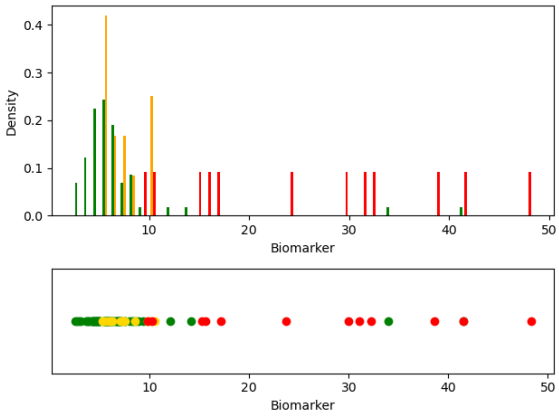

(b) Female

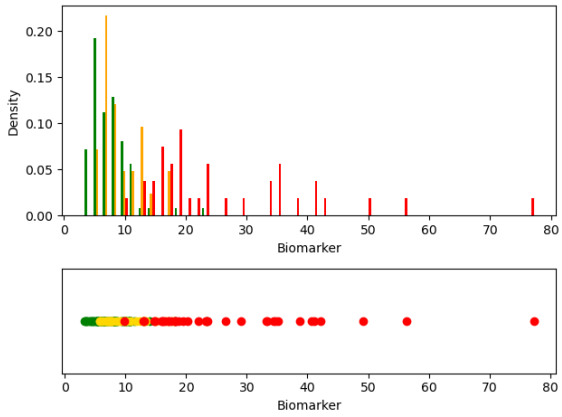

(c) Male

Figure 26: **Single Value Biomarker for Healthy, Prediabetic and Type 2 Diabetic Individuals.** Biomarker is plotted for (a) both genders, (b) females only, and (c) males only. In each subfigure, the x-axis depicts the biomarker value, the y-axis in the histogram represents the histogram density. Red depicts diabetic individuals, yellow depicts prediabetic individuals, and green depicts healthy individuals.

The effect of male and female separation appears to be much more distinct when calculating this biomarker than just observing the parameter values. If the cutoff between healthy and type 2 diabetic females is selected to be 13.0, 4 healthy individuals (corresponding to 6.3% of all healthy individuals) would be predicted to be type 2 diabetic and no diabetic individuals would be predicted to be healthy. For males, if the cutoff is selected to be 17.0, 4 healthy individuals (corresponding to 4.7% of all male healthy individuals) are classified as type 2 diabetic, and 1 diabetic individual is classified as healthy (3.4% of all male diabetic individuals). The one diabetic individual who was below the diabetic cutoff had an HbA1c measurement of 6.9%, OGTT of 199 mg/dL and FBG of 90 mg/dL. This individual is within healthy metrics for their FBG, on the diabetic cutoff for OGTT, and diabetic for HbA1c. 74.8% of all healthy individuals, 72.6% of healthy males, and 61.9% of healthy females were greater than the minimum prediabetic biomarker value.

There is a fairly clear distinction between healthy and diabetic individuals in Figure 25. Apart from a few healthy outliers, as the biomarker increases, the proportion of diabetic individuals also increases. This trend is followed by the prediabetic individuals, who fall in the upper range of the healthy individuals, seen in Figure 26. However, there is not a clear separation of healthy individuals and prediabetic individuals. Thus, another method will be implemented in the next section to better classify individuals into the Healthy, Prediabetic, and Type 2 Diabetic classes.

4.2 Model Parameter Distribution Biomarker

In the previous section, we looked at different parameter summary values for A_1 and A_2. By doing so, we were able to extract a biomarker of diabetic status. However, a main objective of this research was to identify more individuals who may qualify as "prediabetic", or whose glucose homeostasis is slightly abnormal. In this section we propose a new method for the evaluation of glucose homeostasis. Rather than looking at the parameter summary values such as mean, range, and standard deviation, we look at the distribution of the parameters as a whole.

The methodology behind this section is fairly straightforward. First, all the individuals who have diagnostic metrics (HbA1c, OGTT, FBG) were classified as healthy, prediabetic, or T2D using the same protocol as in Chapter 3. Once all the individuals have been placed within the three groups, every parameter value for each individual is used to create a representative parameter distribution for each group. As a result, we end up with representative parameter distributions for the parameters A_1 and A_2 for healthy individuals, representative parameter distributions for prediabetic individuals, and representative parameter distributions for diabetic individuals.

Individuals who were classified as prediabetic in the second Klick Followup study were excluded when creating the representative prediabetic distribution. Numerous sources indicate a discrepancy between HbA1c and OGTT for diagnosing prediabetes, with one source concluding that HbA1c had a sensitivity of 49% and specificity of 79% [29]. This indicates that only 49% of individuals in this review classified as prediabetic from HbA1c were actually prediabetic according to their OGTT. Furthermore, the Stanford study data was excluded, as the gender of all participants was not given. Both the Stanford Study and the second Klick Followup Study will be used for validation after the method is implemented.
Once the representative distributions for the groups were created, they were compared to an individual's parameter distributions. By determining which distribution the individual was closest to, the individual could be classified as either Healthy, Prediabetic, or Diabetic. We are able to compare distributions by

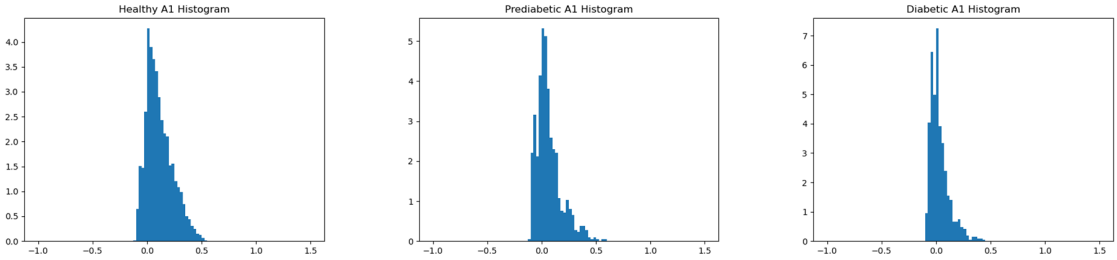

Figure 27: **Representative Parameter Histograms,** A_1.

first converting the three representative parameter distributions for a single parameter and an individual's distribution for the same parameter into cumulative distribution functions (CDF). The area between the individual's CDF and the representative Healthy CDF is calculated numerically by taking the sum across all parameter values of the vertical difference between the two distributions multiplied by the step size. The area is then calculated between the individual's CDF and the representative Prediabetic CDF, and between the individual's CDF and the Diabetic CDF. Whichever group corresponds to the minimum area will be the group that the individual will be classified as. For example, if the area is minimized between the individual and the representative Prediabetic distributions, the individual will be classified as Prediabetic.

4.2.1 A_1 Only

The distribution of the bootstrapped parameter A_1 for diabetic individuals differed the most from the bootstrapped parameter distribution of A_1 for healthy individuals, seen in Tables 3 and 1. As such, this is the parameter we will start with in order to predict diabetic status. The representative distributions can be seen in Figure 27 and the representative CDFs for healthy, prediabetic, and diabetic individuals can be seen in Figure 28.

After the representative distributions have been calculated for males and females, we can begin to compare the individual's parameter distribution for A_1 with the representative distributions. A male individual's A_1 distribution and how it compare to representative distributions in Figure 29. Calculating the distance

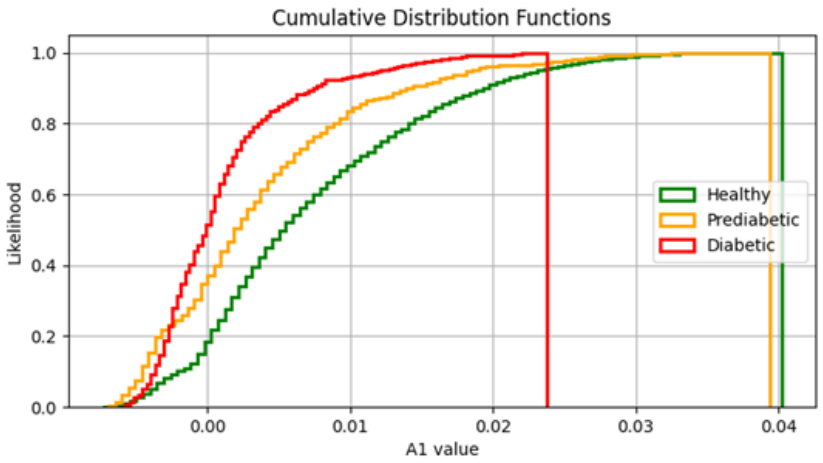

Figure 28: **Representative Parameter Distributions,** A_1.

between the cumulative distribution functions, the distance between the individual and the healthy distribution is 1.4977, 3.2277 between the individual and prediabetic distribution, and 6.9766 between the individual and diabetic distribution. The minimum distance in this example is between the individual and the healthy distribution, therefore the individual would be predicted to be healthy according to their A_1 values.

Looking at two more examples, we can see in Figure 30 (a) an individual who's CDF closely resembles that of the prediabetic distribution. Calculating the area between the curves, the area between the individual CDF and representative healthy CDF was 2.4524, the area was 0.9135 between the individual and the prediabetic distribution, and 3.7609 between the individual and the diabetic population. The minimum area is between the individual and the prediabetic distribution (which can be visually confirmed in Figure 30 (a)), thus the individual would be predicted to be prediabetic. Finally, we have a diabetic male according to their diagnostics. Comparing the distribution to the representative distributions, the area between the individual CDF and the healthy CDF is 5.6155, the area between the individual CDF and prediabetic CDF is 3.5278, and the area between the individual CDF and the diabetic CDF is 1.3513. This can be visually confirmed by the four CDFs in Figure 30 (b). Thus, the individual is predicted to be diabetic, which aligns with the actual diagnosis.

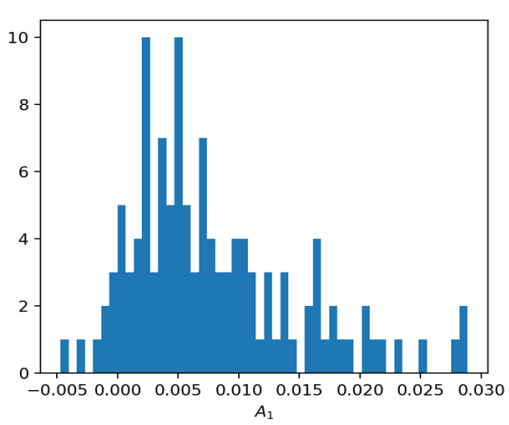

(a) Individual Parameter Distribution

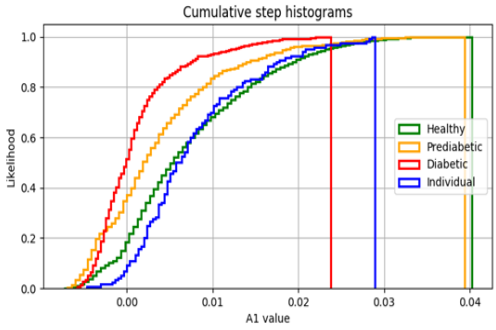

(b) Representative CDF Comparison

Figure 29: A_1 **Parameter Distribution for a Healthy Individual**. Parameter Histogram for the individual is found in (a) and the Comparative Cumulative Distribution Function in (b)

The results of the analysis can be found in Table 5. If we do not split the population into male and female, Healthy classification has a precision and recall of 97.9% and 72.0% respectively. The prediabetic classification has a precision and recall of 15.9% and 62.5%, and the diabetic classification has a precision and recall of 82.7% and 89.6%. A detailed description of precision and recall and their corresponding calculations can be found in Appendix B.

When the CDF analysis is performed on the genders separately, we obtain slightly different results. For females, the healthy precision, prediabetic precision, and diabetic precision is 98.3%, 17.9%, and 80.0% respectively. The recall is 71.1%, 83.3%, and 84.2% for healthy, prediabetic, and diabetic respectively. For males, the healthy precision, prediabetic precision, and diabetic precision is 97.6%, 14.7%, and 81.3% respectively. The recall is 73.6%, 50.0%, and 89.7% for healthy, prediabetic, and diabetic respectively.

4.2.2 A_2 Only

The analysis was repeated using only the A_2 values for each individual. The results of the analysis can be found in Table 6. Looking at the case of no gender separation, Healthy classification has a precision

No Gender Separation			$N = 257$	
		Model Prediction		
Diagnosis	Healthy	Prediabetic	Diabetic	**Recall**
Healthy ($N = 193$)	139	48	6	0.720
Prediabetic ($N = 16$)	3	10	3	0.625
Diabetic ($N = 48$)	0	5	43	0.896
Precision	0.979	0.159	0.827	
Females Only			$N = 149$	
		Model Prediction		
Diagnosis	Healthy	Prediabetic	Diabetic	**Recall**
Healthy ($N = 83$)	59	20	4	0.711
Prediabetic ($N = 6$)	1	5	0	0.833
Diabetic ($N = 19$)	0	3	16	0.842
Precision	0.983	0.179	0.800	
Males Only			$N = 108$	
		Model Prediction		
Diagnosis	Healthy	Prediabetic	Diabetic	**Recall**
Healthy ($N = 110$)	81	26	3	0.736
Prediabetic ($N = 10$)	2	5	3	0.500
Diabetic ($N = 29$)	0	3	26	0.897
Precision	0.976	0.147	0.813	

Table 5: Results of Parameter Distribution Biomarker, A_1 Only

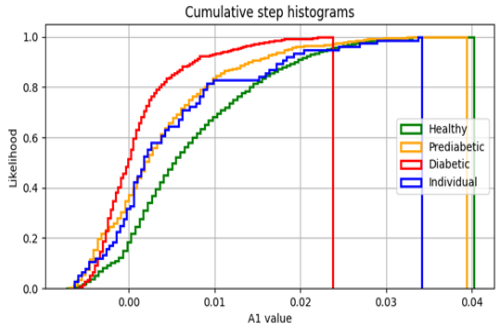

(a) Prediabetic Prediction

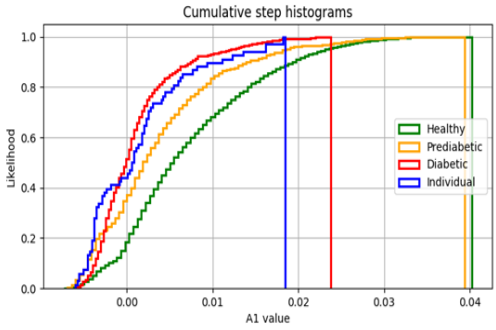

(b) Diabetic Prediction

Figure 30: A_1 **Parameter Distribution for Prediabetic and Diabetic Individuals**.

and recall of 99.1% and 57.0% respectively. The prediabetic classification has a precision and recall of 10.6% and 56.3%, and the diabetic classification has a precision and recall of 52.5% and 66.7%.

When the CDF analysis is performed on the genders separately, we obtain slightly different results. For females, the healthy precision, prediabetic precision, and diabetic precision is 100.0%, 14.2%, and 50.0% respectively. The recall is 65.1%, 66.7%, and 68.4% for healthy, prediabetic, and diabetic respectively. For males, the healthy precision, prediabetic precision, and diabetic precision is 100.0%, 11.5%, and 52.8% respectively. The recall is 55.45%, 60.0%, and 65.5% for healthy, prediabetic, and diabetic respectively.

4.2.3 A_1 and A_2

After collecting the results from the CDF analysis independently for the A_1 and A_2 parameters, they will now need to be combined in order to get a more comprehensive prediction of diabetic status. This will be performed using the equation below:

$$k_1\mathbf{B} + k_2\mathbf{C} = \mathbf{D}$$

Where $\mathbf{B}$ is a vector containing the area between the individual and the healthy CDF for the parameter A_1, the area between the individual and the prediabetic CDF for the parameter A_1, and the area between

No Gender Separation			$N = 257$	
		Model Prediction		
Diagnosis	Healthy	Prediabetic	Diabetic	**Recall**
Healthy ($N = 193$)	110	60	23	0.570
Prediabetic ($N = 16$)	1	9	6	0.563
Diabetic ($N = 48$)	0	16	32	0.667
Precision	0.991	0.106	0.525	
Females Only			$N = 149$	
		Model Prediction		
Diagnosis	Healthy	Prediabetic	Diabetic	**Recall**
Healthy ($N = 83$)	54	18	11	0.651
Prediabetic ($N = 6$)	0	4	2	0.667
Diabetic ($N = 19$)	0	6	13	0.684
Precision	1.000	0.143	0.500	
Males Only			$N = 108$	
		Model Prediction		
Diagnosis	Healthy	Prediabetic	Diabetic	**Recall**
Healthy ($N = 110$)	61	36	13	0.554
Prediabetic ($N = 10$)	0	6	4	0.600
Diabetic ($N = 29$)	0	10	19	0.655
Precision	1.000	0.115	0.528	

Table 6: Results of Parameter Distribution Biomarker, A_2 Only

the individual and the diabetic CDF for the parameter A_1. **C** is a vector containing the areas between the individual and the representative CDFs for the parameter A_2, **D** is a vector containing the linear combinations of the areas, and k_1 and k_2 are parameters. k_1 and k_2 will be the same for all individuals (i.e. will not vary person to person). Expanded, the equation becomes:

$$k_1 \begin{bmatrix} A_1 \text{ Area to Healthy} \\ A_1 \text{ Area to Prediabetic} \\ A_1 \text{ Area to Diabetic} \end{bmatrix} + k_2 \begin{bmatrix} A_2 \text{ Area to Healthy} \\ A_2 \text{ Area to Prediabetic} \\ A_2 \text{ Area to Diabetic} \end{bmatrix} = \begin{bmatrix} \text{Total Area to Healthy} \\ \text{Total Area to Prediabetic} \\ \text{Total Area to Diabetic} \end{bmatrix}$$

Which will be denoted as:

$$k_1 \begin{bmatrix} b_H \\ b_P \\ b_D \end{bmatrix} + k_2 \begin{bmatrix} c_H \\ c_P \\ c_D \end{bmatrix} = \begin{bmatrix} d_H \\ d_P \\ d_D \end{bmatrix}$$

The predicted diabetic status for each individual will be the class corresponding to the minimum value in vector **D**. For example, if after computing the linear combination,

$$\mathbf{D} = \begin{bmatrix} 1.1 \\ 0.6 \\ 2.4 \end{bmatrix}$$

the individual would be predicted to be prediabetic. The absolute areas computed for the A_2 parameter analysis were smaller than the areas computed for the A_1 parameter, so the values will be scaled before computing the linear combination. This was done by converting all the values within **B** and **C** to values between 0 and 1, and all the values within **B** and **C** will correspondingly sum to 1. This was done by dividing each element within **B** and **C** by the sum of all the elements in **B** if the element is in **B** or the sum of all the elements in **C** if the element is in **C**.

k_1 and k_2 were determined by finding the values that minimize the number of incorrect diagnoses. "Incorrect diagnoses" in this context would be an individual with impaired glucose homeostasis (i.e.

Prediabetic or Diabetic by the diagnostic criteria) who were classified as healthy, or healthy individuals who were classified as Prediabetic or Type 2 Diabetic. No error was given to Prediabetic individuals who were classified as Type 2 Diabetic, or for T2D individuals who were classified as Prediabetic, as one of the intended outcomes for this method is to be used as a screening tool for impaired glucose homeostasis without having to do blood tests or schedule an appointment with a physician. The number of incorrect diagnoses were calculated for values between -0.1 and 5 with a step size of 0.01 for both k_1 and k_2 for the case in which the genders were not separated, and for when the analysis for females and males were performed separately. It was determined that the minimum incorrect prediabetic diagnoses for when the genders were not separated was 6 individuals, for females it was 1 individual, and for males it was 4 incorrect individuals. The optimized k_1 and k_2 values, in order for no gender separation, females only, and males only, were $k_1 = 2.85$ and $k_2 = 0.27$, $k_1 = 3.0$ and $k_2 = 2.1$, and $k_1 = 0.5$ and $k_2 = 3.0$.

The results of the analysis can be found in Table 7. Looking at the case of no gender separation, Healthy classification has a precision and recall of 97.2% and 72.5% respectively. The prediabetic classification has a precision and recall of 15.0% and 56.3%, and the diabetic classification has a precision and recall of 81.1% and 89.6%.

When the CDF analysis is performed on the genders separately, we obtain slightly different results. For females, the healthy precision, prediabetic precision, and diabetic precision is 98.4%, 17.9%, and 84.2% respectively. The recall is 72.3%, 83.3%, and 84.2% for healthy, prediabetic, and diabetic respectively. For males, the healthy precision, prediabetic precision, and diabetic precision is 98.8%, 18.2%, 81.3% respectively. The recall is 75.5%, 60.0%, and 89.7% for healthy, prediabetic, and diabetic respectively.

No Gender Separation			$N = 257$	
		Model Prediction		
Diagnosis	Healthy	Prediabetic	Diabetic	**Recall**
Healthy ($N = 193$)	140	46	7	0.725
Prediabetic ($N = 16$)	4	9	3	0.563
Diabetic ($N = 48$)	0	5	43	0.896
Precision	0.972	0.150	0.811	
Females Only			$N = 149$	
		Model Prediction		
Diagnosis	Healthy	Prediabetic	Diabetic	**Recall**
Healthy ($N = 83$)	60	20	3	0.723
Prediabetic ($N = 6$)	1	5	0	0.833
Diabetic ($N = 19$)	0	3	16	0.842
Precision	0.984	0.179	0.842	
Males Only			$N = 108$	
		Model Prediction		
Diagnosis	Healthy	Prediabetic	Diabetic	**Recall**
Healthy ($N = 110$)	83	24	3	0.755
Prediabetic ($N = 10$)	1	6	3	0.600
Diabetic ($N = 29$)	0	3	26	0.897
Precision	0.988	0.182	0.813	

Table 7: Results of Parameter Distribution Biomarker, Combination A_1 & A_2

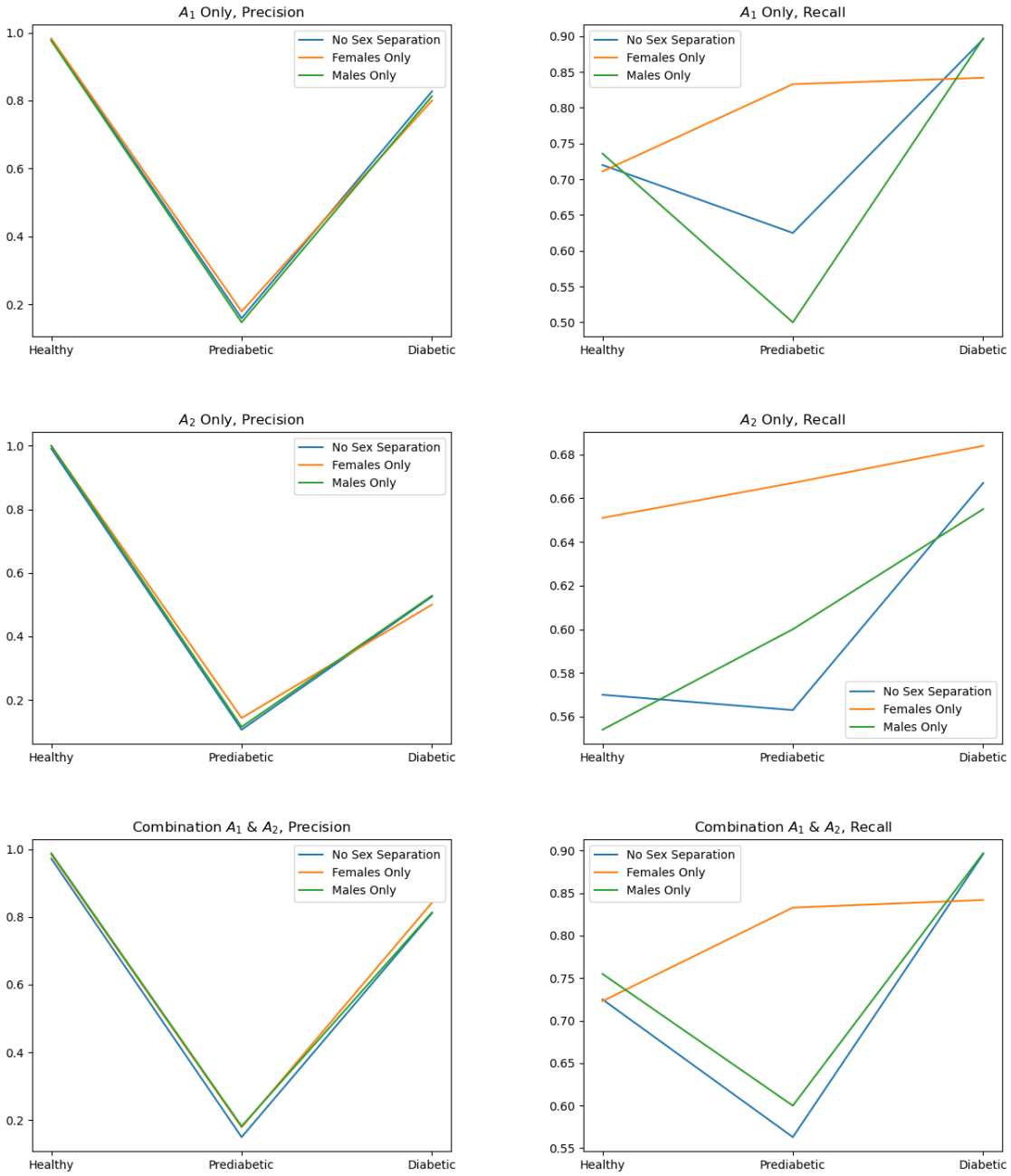

Figure 31: **Graphical Representation of Precision and Recall Between Diagnostics**.

Prediabetic and diabetic diagnoses can be pooled into a single class (Impaired Glucose Homeostasis, IGH) and the precision and recall can be evaluated. Results can be seen in 8. If the genders are not separated, the precision and recall are 97.2% and 72.5% for healthy, and 53.1% and 93.8% for IGH. For the female only analysis, the precision and recall are 98.4% and 72.3% for healthy, and 51.1% and 96.0% for IGH. For the male only analysis, the precision and recall are 98.8% and 75.5% for healthy, and 58.5% and 97.4% for IGH.

Starting with the "No Gender Separation" Case in Table 8, the individuals who were misclassified can be evaluated. For the four individuals classified as healthy but have impaired glucose homeostasis, two individuals had OGTT readings that were close to the healthy cutoff (144 and 150 mmol/L), and healthy FBG (both 93 mmol/L) and HBA1c levels (5.2% and 5.5%). For the other two individuals misclassified as healthy, the OGTT levels were within healthy ranges (131 and 120 mmol/L), with prediabetic FBG (102 and 104 mmol/L) and HbA1c (6.7% and 7.1%). For the individuals misclassified as IGH, 30 were individuals who exclusively had HbA1c measurements (no FBG or OGTT). HbA1c studies have shown it to have a specificity of 21% for prediabetic individuals, indicating that 21% of individuals classified as healthy according to HbA1c were actually prediabetic [29]. 21% of healthy individuals who only had an HbA1c reading was 28.56, so 30 individuals predicted to be prediabetic is right in line with expected values. 10 individuals misclassified as IGH were within prediabetic levels for either FBG or HbA1c, and the remaining 13 individuals had no indication of impaired glucose homeostasis from their diagnostic metrics.

For the analysis on female participants, the one individual misclassified as healthy had a borderline OGTT (144 mmol/L), and healthy FBG and HbA1c (93 mmol/L and 5.2% respectively). Of the 23 individuals misclassified as IGH, 12 of them exclusively had HbA1c (no OGTT or FBG), which corresponds to 21.8% of all healthy female individuals. This is in line with the expected 21% of healthy individuals according to HbA1c actually being prediabetic [29]. 6 individuals were within prediabetic levels for one of FBG or HbA1c, and the remaining 5 individuals had no indication of prediabetes from their diagnostic metrics.

No Gender Separation			$N = 257$
	Model Prediction		
Diagnosis	Healthy	IGH	**Recall**
Healthy ($N = 193$)	140	53	0.725
IGH ($N = 64$)	4	60	0.938
Precision	0.972	0.531	

Females Only			$N = 108$
	Model Prediction		
Diagnosis	Healthy	IGH	**Recall**
Healthy ($N = 83$)	60	23	0.723
IGH ($N = 25$)	1	24	0.960
Precision	0.984	0.511	

Males Only			$N = 149$
	Model Prediction		
Diagnosis	Healthy	IGH	**Recall**
Healthy ($N = 110$)	83	27	0.755
IGH ($N = 39$)	1	38	0.974
Precision	0.988	0.585	

Table 8: Results of Parameter Distribution Biomarker, Combination A_1 & A_2. IGH is Impaired Glucose Homeostasis.

For the analysis on male participants, the individual misclassified as healthy had a borderline prediabetic OGTT (150 mmol/L) and healthy FBG and HbA1c (93 mmol/L and 5.5% respectively). Of the 27 individuals classified as IGH, 15 of them only had an HbA1c measurement (17.4 % of healthy individuals with only HbA1c reading), and 4 individuals had either a prediabetic FBG reading or HbA1c. The remaining 8 males had no indication of prediabetes or impaired glucose homeostasis according to their diagnostic metrics.

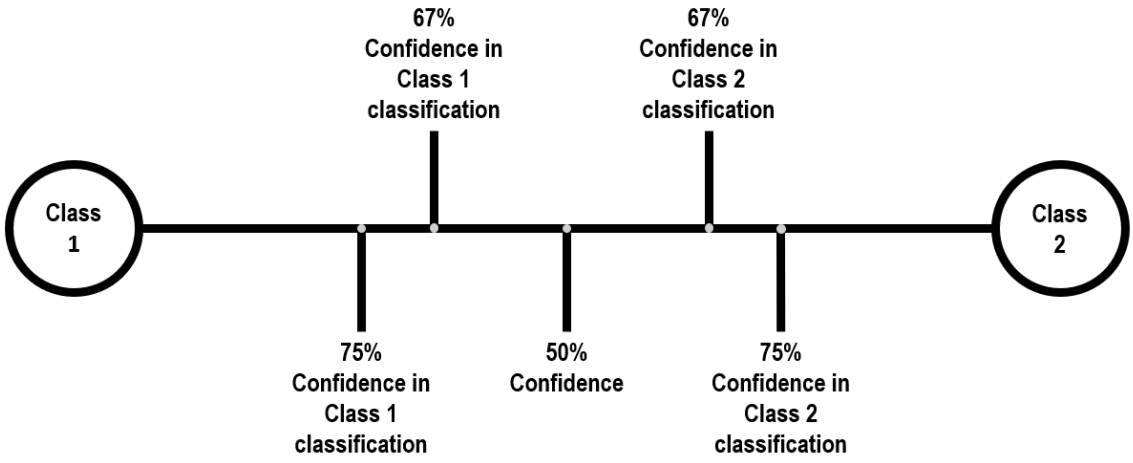

Figure 32: **Confidence Score Schematic**

4.2.4 Confidence Calculation

An additional feature that can be added to the analysis is a confidence score, or how confident the classification is that the prediction is correct. This was implemented by creating a score between 0.5 (50% confident) and 1.0 (100% confident) for each classification. If the confidence score was 0.5, the individual was equidistant to two classes, or equally likely to be a part of either class, and if the confidence score is 1.0, the individual distribution was exactly equal to the predicted class distribution. Furthermore, if the closest distance was half of the next closest distance, the confidence score was 0.67, and if the closest distance was one third the distance of the next closest distance, the confidence score was 0.75. This is demonstrated in Figure 32. The confidence score was calculated as follows:

$$\text{Confidence Score} = \frac{1}{2}\frac{d_2 - d_1}{d_2 + d_1} + \frac{1}{2}$$

Where d_1 is the smallest area of the individual distribution to the representative distributions and d_2 is the second smallest area.

When this score is applied to the method, the misclassified individuals can be evaluated further. Of the 13 individuals in the implementation where gender was not separated, "Prediabetic" was the closest distribution and "Healthy" was the next prediction for 11 individuals, and all confidence scores were under 75%. For the 5 females without an indication of glucose homeostasis dysfunction, 4 of them had "Prediabetic" as the closest distribution and "Healthy" as the next closest distribution, and all the confidence scores were below 70%. One individual had "Prediabetic" as the closest distribution and "Diabetic" as the next closest with a confidence score of 74%. For the 8 males who had no indication of glucose homeostasis dysfunction, 5 individuals were predicted to be "Prediabetic" with the next closest distribution "Healthy" and confidence scores below 70%. 2 individuals were predicted to be "Prediabetic" with "Diabetic" as their next prediction, and 1 individual was predicted to be "Diabetic".

4.2.5 Extension

Now that the biomarker method has been implemented with the above data, it can be tested on the excluded Stanford Study data and individuals who were within prediabetic ranges for their HbA1c, but did not have other metrics to validate. The results of the Stanford Study Biomarker analysis can be found in Table 9. The parameter values were set to be equal to the optimized parameter values determined in the previous section, so that $k_1 = 2.85$ and $k_2 = 0.27$.

The results of individuals classified as prediabetic according to HbA1c can be seen in Table 10. The parameter values were kept the same as calculated previously, so for no gender separation, females only, and males only, $k_1 = 2.85$ and $k_2 = 0.27$, $k_1 = 3.0$ and $k_2 = 2.1$, and $k_1 = 0.5$ and $k_2 = 3.0$ respectively.

No Gender Separation, Stanford				$N = 54$
		Model Prediction		
Diagnosis	Healthy	Prediabetic	Diabetic	**Recall**
Healthy ($N = 39$)	16	21	2	0.410
Prediabetic ($N = 11$)	0	5	6	0.455
Diabetic ($N = 4$)	0	1	3	0.750
Precision	1.000	0.185	0.273	

Table 9: Results of Parameter Distribution Biomarker, Combination A_1 & A_2, Stanford Study.

No Gender Separation				
		Model Prediction		
Diagnosis	Healthy	Prediabetic	Diabetic	**Recall**
Prediabetic ($N = 50$)	17	24	9	0.480
Females Only				
		Model Prediction		
Diagnosis	Healthy	Prediabetic	Diabetic	**Recall**
Prediabetic ($N = 12$)	5	6	1	0.500
Males Only				
		Model Prediction		
Diagnosis	Healthy	Prediabetic	Diabetic	**Recall**
Prediabetic ($N = 38$)	12	18	8	0.474

Table 10: Results of Parameter Distribution Biomarker, Combination A_1 & A_2, HbA1c indicated Prediabetic.

No Gender Separation, Stanford			$N = 54$
	Model Prediction		
Diagnosis	Healthy	IGH	**Recall**
Healthy ($N = 39$)	16	23	0.410
IGH ($N = 15$)	0	15	1.000
Precision	1.000	0.395	

Table 11: Results of Parameter Distribution Biomarker, Combination A_1 & A_2, Stanford Study Impaired Glucose Homeostasis (IGH).

The prediabetic and diabetic groups can again be combined to form the "Impaired Glucose Homeostasis" group. Results can be seen in Table 11 and 12. For the Stanford dataset in Table 11, precision was 100.0% for healthy individuals, and 39.5% for prediabetic individuals. Recall was 41.0% for healthy individuals and 100.0% for prediabetic individuals.

For the prediabetic individuals defined by their HbA1c in Table 12, the accuracy of the prediabetic classification was 66.0% for the case in which genders were not separated, 53.8% accurate for females, and 68.4% accurate for males.

No Gender Separation, HbA1c Prediabetic			
		Model Prediction	
Diagnosis	Healthy	IGH	**Recall**
Prediabetic ($N = 50$)	17	33	0.667
Females Only			
		Model Prediction	
Diagnosis	Healthy	IGH	**Recall**
Prediabetic ($N = 12$)	5	7	0.583
Males Only			
		Model Prediction	
Diagnosis	Healthy	IGH	**Recall**
Prediabetic ($N = 38$)	12	26	0.684

Table 12: Results of Parameter Distribution Biomarker, Combination A_1 & A_2, HbA1c indicated Prediabetic, Impaired Glucose Homeostasis (IGH).

4.3 Discussion

The main objective of the thesis was to use the parameter results from model fitting as a metric to classify individuals as prediabetic or type 2 diabetic. Both methods implemented in this section provide a reasonable biomarker for glucose homeostasis and diabetic status classification for individuals with Type 2 Diabetes. However, both methods have their limitations and inaccuracies.

Starting with the single value biomarker, the implementation was very effective at separating individuals with a normal glycemic profile from those with type 2 diabetes, particularly for when genders are separated. The one type 2 diabetic male that did appear to be in diabetic biomarker range had conflicting diagnostics (one healthy, one prediabetic, one diabetic), so it is entirely possible that the biomarker value being within healthy/ prediabetic ranges was accurate. For the most part, as the biomarker value increased, the diabetic status of the individual also increased, where individuals on the left were more likely to be healthy and individuals on the right were diabetic. Prediabetic individual biomarker values are between the healthy and diabetic biomarker values, with most prediabetic individuals falling in the upper range of normal. However, predicting more incidences of prediabetes was less effective, as more than 70% of healthy individuals would be predicted to be prediabetic if the minimum biomarker value was used. Although this is potentially useful for pre-screening purposes and providing a continuous metric of glucose homeostasis, it isn't very practical to assume more than half of the healthy population is actually prediabetic.

Physiologically, there is not much difference between an individual who has an OGTT result of 199 and 201 [30]. However, the first individual would be classified as "Prediabetic" according to medical guidelines for OGTT results, and the second individual would be classified as "Type 2 Diabetic". The thresholds for OGTT were set based off of a statistical increase in risk of adverse outcomes, such as increased morbidity or mortality [31]. So, the lack of complete separation between individuals is to be expected. Furthermore, there was no standardization between participants in terms of study protocol -

all individuals just lived their lives normally and ate anything they wanted during the two week study, compared to tests like OGTT that have a standardized time and glucose amount. Type 2 diabetes can be regulated through diet [32], so if an individual was diagnosed diabetic through the diagnostic metrics but limited their sugar intake during the course of the study, they may appear to have a "more effective" glucose homeostasis than an individual who had healthy diagnostics but ate sugar continuously for the two week period.

For the parameter distribution biomarker, results improved for each iteration of the method that was implemented. Implementing the combination of A_1 and A_2 distance prediction resulted in a higher precision and accuracy for all classes, and fewer individuals with impaired glucose homeostasis (prediabetic or diabetic) were predicted to be healthy. Further method implementation of a confidence score was also effective. Of the total number of incorrect predictions, 87.6% had the correct class as the second closest prediction, with less than 75% confidence in the first predicted class.

Prediabetic and diabetic individuals were successfully separated from the healthy population for 93.3% (no gender separation), 95.0% (female only analysis), and 97.4% (male only analysis) of prediabetic and T2D individuals in the final implementation of the parameter distribution biomarker. A significant proportion of healthy individuals were classified as having impaired glucose homeostasis. For females, 27.7 % of healthy individuals were classified as prediabetic or diabetic, 24.5% of healthy males were classified as prediabetic or diabetic and 27.5 % healthy individuals were classified as prediabetic or diabetic for the analysis that did not separate by gender. Comparing this to the single-value biomarker, where no gender separation, males, and females had 74.8%, 72.6%, and 61.9% respectively of healthy individuals within prediabetic range (above the minimum prediabetic biomarker value), the parameter distribution biomarker is much more effective and distinguishing between the two classes. Male and female separation while performing the analysis had a much more distinct effect in the parameter distribution biomarker results. Precision and recall for all classes increased compared to the analysis that did not separate based on gender. One particular benefit to separating the genders was that fewer prediabetic individuals were

misclassified as healthy.

The intention of this work was to create a screening tool that would be an easy way to predict dysfunctional glucose homeostasis. A high number of false negatives would invalidate the results, more so than a larger proportion of false positives. A false positive gives the individual the impression that they are free from a disease, and are less likely to follow up with a more accurate test (in the case of glucose homeostasis, an OGTT) [33]. Not only does this delay diagnosis, but it increases the risk of morbitity or mortality from the disease [31, 34]. False negatives may also lead to lawsuits depending on the severity and outcomes of a disease [33]. On the other hand, false positives may result in unnecessary visits to the physician and more invasive diagnostic tests. False positives may also increase an individual's psychological stress unnecessarily [33].

Ideally, a screening tool has a sensitivity (proportion of true positives) and specificity (proportion of true negatives) of 1.0. However, these value is rarely achieved by today's screening tools [33]. When looking specifically at the case of type 2 diabetes screening, a high sensitivity is much more important than a high specificity, as it is much less costly to flag individuals with potentially having diabetes than to miss the cases altogether [35]. The sensitivity and specificity of the parameter distribution biomarker method are the recall for individuals with impaired glucose homeostasis and healthy individuals respectively. In all cases (gender separation vs no gender separation), sensitivity was greater than 0.9 (for the cases of gender separation it was greater than 0.95), and specificity was greater than 0.7. This is in line with current screening tests for various diseases [33]. For type 2 diabetes diagnostic metrics in particular, compared to OGTT, HbA1c identifies diabetic individuals with a sensitivity 50% (95% CI: 42–59%) and 97% (95% CI: 95–98%) [36], and the sensitivity and specificity of prediabetes using HbA1c is even worse at 49% (95% CI: 40-58%) and 79% (95% CI: 73-84%) [29]. FBG identifies diabetic individuals with a sensitivity of 59.4% (95% CI: 46.6–71%) and specificity of 98.8% (95% CI: 96.5–99.6%) compared to OGTT [36]. Prediabetic individuals are identified using FBG with a sensitivity of 25% (95% CI: 19-32%) and specificity of 94% (95% CI: 92-96%) [37]. Compared to the two existing metrics,

the parameter distribution biomarker method is much more sensitive and slightly less specific, which will flag more individuals as being at risk for type 2 diabetes but will not miss as many individuals who actually have glucose homeostasis dysfunction. Additionally, CGM devices are much less invasive than going to a physician and doing a blood test, and data can be collected as individuals go about their daily routines. As such, the parameter distribution biomarker appears to be a viable screening tool for type 2 diabetes and prediabetes.

The analysis performed on the participants of the Stanford Study had mixed results. The method (using the optimized parameters for the test data set) had a precision of 1.0 for healthy classification, so no individuals were predicted to be healthy who were not actually healthy. However, a much higher proportion of healthy individuals were predicted to be prediabetic or diabetic, consisting of 59.0% of healthy individuals predicted to have some form of dysfunctional glucose homeostasis. Again, it is not practical to flag this many individuals as being at risk for type 2 diabetes, so more refinement of the technique is needed to increase the specificity. That being said, of the 23 healthy individuals incorrectly labelled as prediabetic or diabetic, 20 participants (86.9% of all mislabelled healthy individuals) had the correct class as the second closest prediction, with less than 75% confidence in the first predicted class. Furthermore, 14 of the 23 participants (60.9%) had a confidence score below 60%.

When looking at the individuals with prediabetic HbA1c metrics (but no other diagnostic methods), the accuracy of the results of the parameter distribution biomarker appear low, with only 48 % of individuals being classified as prediabetic for the case of no gender separation, 50 % of individuals classified as prediabetic for the female-only analysis, and 47% of individuals classified as prediabetic for the male-only analysis. However, HbA1c alone has been shown to have a 0.49 sensitivity (95% CI 0.40 and 0.58), indicating that HbA1c alone will accurately predict prediabetes only 49% of the time [29]. Thus, the proportion of prediabetic predictions are right in line with expected values. In order to be confident that the proportions are accurately representative of the sample population, further tests would have to be performed on these individuals (such as OGTT) to confirm.

In both the single value biomarker and the parameter distribution biomarker, it was difficult to distinguish between healthy individuals and prediabetic individuals. This may in part be due to the definition of prediabetes. Prediabetic individuals have glycemic results that are above normal but below type 2 diabetic thresholds. Although there are some risk factors associated with this division of individuals (such as nephropathy and increased risk of macrovascular disease), it is essentially just a high risk state for type 2 diabetes. Annually, 5-10% of individuals with prediabetes will progress to type 2 diabetes, but a similar quantity will convert back to normal glycemic levels [32]. Furthermore, the ADA estimated that up to 70% of individuals with prediabetes will eventually develop type 2 diabetes, however there is a 40-70% reduction of risk of progressing to type 2 diabetes if the individual undergoes a lifestyle modification to increase exercise and eat healthier [32]. There is no way to determine if a prediabetic individual in this study will progress to type 2 diabetes or revert back to normal without following them and their diabetic status in a longitudinal study.

One difficulty that emerged when working with individuals with impaired glucose homeostasis was the lack of a "ground truth". Diabetes guidelines provide the thresholds for traditional diagnostic methods such as OGTT, HbA1c, and FBG. However, these metrics can indicate conflicting results. For example, a few individuals in the first Klick Followup Study were healthy in one metric, prediabetic in another, and diabetic in a third. Specifically, one individual had an OGTT of 131 mg/dL (within healthy range), FBG of 102 mg/dL (within prediabetic range) and HbA1c of 6.7% (within diabetic range). Just looking at the diagnostic metrics does not provide the diabetic status of the individual, and the diagnostics may contradict each other. A biomarker that is correlated with multiple diagnostic methods may be useful in evaluating these more ambiguous cases.

Up to 50% of individuals with diabetes have not been diagnosed, and some individuals may remain undiagnosed for up to 12 years [38]. This implementation, either the single value biomarker or the parameter distribution biomarker, may be useful in this case as a screen. If the results give "Prediabetic"

or “Diabetic”, the individual could schedule an appointment with a physician in order to take an OGTT and give a more accurate classification and diagnosis.

5 Conclusion

5.1 Model Potential

Overall, there is definite promise to using a proportional-integral controller to mathematically model an individual's glucose homeostasis. Two biomarkers of diabetic status and glucose homeostasis function were created from parameter results obtained from model fitting. It was shown that these biomarkers have reasonable accuracy and are able to separate healthy individuals from individuals with impaired glucose homeostasis. The most inaccurate part of both biomarker methods was incorrectly identifying too many healthy individuals as prediabetic or diabetic. However, if this method was indeed implemented as a pre-screen for glucose homeostasis, fewer individuals who were actually prediabetic or type 2 diabetic would be missed, and healthy individuals who may be borderline prediabetic may be identified sooner.

The benefit to this implementation is the convenience of the analysis and results. The procedure is almost completely non-invasive, with the individual only having to put on a CGM and not be subjected to any blood tests for glucose readings or hormone levels. There is no need for the individual to fast or be subjected to any other food restrictions, and the individual can carry out their day-to-day life as normal. Additionally, the analysis can be performed locally on a personal device or computer. This will allow more individuals to evaluate their own glucose homeostasis and determine if they should seek the professional opinion of a physician. The aim would be to screen more individuals for being at risk for type 2 diabetes and begin prevention as early as possible to prevent disease progression.

5.2 Limitations

There are a few limitations for using a CGM method as a potential diagnostic or screening tool for T2D and prediabetes. In the current way that the model is implemented, there is no standardized meals or

sugar intake for participants. This has the benefit of not disrupting an individual's day-to-day life, however the overlap between healthy individuals and prediabetic individuals may start to be more obvious. It may be beneficial to apply the model to a standardized procedure in order to evaluate the differences in model fit.

Another limitation of this research was the disproportionate representation of healthy individuals in the analysis. The intention of the data collection was to have a even split of healthy, prediabetic, and diabetic individuals, but with the screening method implemented to enroll participants (CANRISK score for diabetic risk) the enrollment tended to be heavily skewed towards healthy individuals.

A final limitation of the research was the data collection location. The data collected in the two Klick Followup studies was exclusively collected from individuals from India. Although the Klick Pilot study was collected from Toronto, Ontario and the Stanford dataset was collected from individuals in California, USA, the majority of individuals was from a specific region and demographic. No discrepancies were observed between datasets, but it would be beneficial to evaluate more individuals from other regions of the world.

5.3 Future Work

Future work for this project involves fine-tuning the procedures and implementation of the biomarker methods. One avenue to pursue is implementing a machine learning approach to find the ideal cutoffs for the single-value biomarker and find the parameters that minimize the incorrect predictions for the parameter distribution biomarker. Another feature that can be added to the analysis is implementing a way to incorporate an individual's average glucose values or glucose baseline in the parameter distribution biomarker in an attempt to obtain a better specificity.

Furthermore, it would be interesting to conduct a longitudinal observational study to evaluate how

an individual's homeostasis would evolve over time. This study could also be used to compare the current biomarkers to diabetes progression or regression back to normal glycemic activity. Additionally, interventions could be evaluated for effectiveness if biomarker values change before and after intervention implementation.

Finally, the homeostasis profiles could be evaluated and the individuals could potentially be grouped into different clusters depending on their model results. The idea behind this stems from the possibility that some individuals may be more likely to experience glucose homeostasis dysfunction if they are a member of a specific group.

Appendices

A Bootstrapping

Bootstrapping is the term used to describe any metric or calculation that uses random sampling with replacement. When taking the bootstrap mean, a subpopulation of N data points was randomly sampled with replacement from the whole population. The arithmetic mean was calculated from this subpopulation and stored. This process was repeated M times. After the random sampling was repeated, the arithmetic mean of the means calculated from the subpopulations was calculated. This final calculation represents the bootstrap average.

The method employed in this study calculates the bootstrap average for each individual in an attempt to reduce any outlier peaks or model fitting. After doing the calculation, the resulting summary statistic will give a more robust depiction of the individual parameter means.

For each individual, the number of data points that were randomly sampled with replacement, N, was equal to the number of selected peaks, or the length of the array containing the parameter values. M, or the number of times the process was repeated, was set to be equal to 20.

B Accuracy, Precision & Recall

Before discussing precision and recall in classification, it is important to understand the difference between true positives, true negatives, false positives and false negatives. A true positive is when both the predictive value and the actual value are positive, or when the data point is correctly classified as positive. A true negative is when both the predictive value and the actual value are negative, or when the data point is correctly classified as negative. A false positive is when the actual value is negative but the predicted value is positive. A false negative when the actual value is positive but the predicted value is negative. Take for example, the classification of individuals with type 2 diabetes and individuals without type 2 diabetes (i.e. healthy individuals and prediabetic individuals). A true positive would occur when the classification correctly identifies an individual with type 2 diabetes. A true negative would occur when the classification correctly identifies an individual without type 2 diabetes. A false positive would occur when the classification incorrectly predicts someone to have type 2 diabetes when they do not, and a false negative would occur when the classification incorrectly predicts someone to not have type 2 diabetes when they actually do have type 2 diabetes.

One of the most common ways to analyze a classification problem is to calculate the accuracy. The accuracy is defined as the proportion of true positives and true negatives to the total number of individuals. This can be calculated as follows:

$$\text{Accuracy} = \frac{t_p + t_n}{t_p + t_n + f_p + f_n}$$

Where tp is the number of true positives, tn is the number of false negatives, fp is the number of false positives, and fn is the number of false negatives. This metric summarizes the total number of correct predictions by the classification.

Other common ways to analyze the effectiveness of the classification is to calculate the precision and

recall. Recall is the true positive rate, or the sensitivity of the classification, and is calculated as follows:

$$\text{Recall} = \frac{t_p}{t_p + f_n}$$

Precision is the positive predictive value. This calculates the proportion of positive results that are true positives in the calculation, and is calculated as follows:

$$\text{Precision} = \frac{t_p}{t_p + f_p}$$

References

[1] W. B. Cannon, "Physiological regulation of normal states: some tentative postulates concerning biological homeostatics," *Ses Amis, ses Colleges, ses Eleves*, 1926.

[2] H. Modell, W. Cliff, J. Michael, J. McFarland, M. P. Wenderoth, and A. Wright, "A physiologist's view of homeostasis," *Advances in physiology education*, 2015.

[3] J. E. Gerich *et al.*, "Physiology of glucose homeostasis.," *Diabetes, Obesity and Metabolism*, vol. 2, no. 6, pp. 345–350, 2000.

[4] P. Mathew and D. Thoppil, "Hypoglycemia," *StatPearls [Internet]*, 2021.

[5] M. Mouri and M. Badireddy, "Hyperglycemia," *StatPearls [Internet]*, 2021.

[6] J. F. Ndisang, A. Vannacci, and S. Rastogi, "Insulin resistance, type 1 and type 2 diabetes, and related complications 2017," 2017.

[7] "Type 2 diabetes." https://www.cdc.gov/diabetes/basics/type2.html, Dec 2021.

[8] A. D. Association, "Economic costs of diabetes in the us in 2017," *Diabetes care*, vol. 41, no. 5, pp. 917–928, 2018.

[9] "Prediabetes - your chance to prevent type 2 diabetes." https://www.cdc.gov/diabetes/basics/prediabetes.html, Dec 2021.

[10] R. Lin, F. Brown, S. James, J. Jones, and E. Ekinci, "Continuous glucose monitoring: A review of the evidence in type 1 and 2 diabetes mellitus," *Diabetic Medicine*, vol. 38, no. 5, p. e14528, 2021.

[11] X. Yu, L. Lin, J. Shen, Z. Chen, J. Jian, B. Li, and S. X. Xin, "Calculating the mean amplitude of glycemic excursions from continuous glucose data using an open-code programmable algorithm based on the integer nonlinear method," *Computational and mathematical methods in medicine*, vol. 2018, 2018.

[12] F. Gude, P. Díaz-Vidal, C. Rúa-Pérez, M. Alonso-Sampedro, C. Fernández-Merino, J. Rey-García, C. Cadarso-Suárez, M. Pazos-Couselo, J. M. García-López, and A. Gonzalez-Quintela, "Glycemic variability and its association with demographics and lifestyles in a general adult population," *Journal of diabetes science and technology*, vol. 11, no. 4, pp. 780–790, 2017.

[13] J. R. Sparks, E. E. Kishman, M. A. Sarzynski, J. M. Davis, P. W. Grandjean, J. L. Durstine, and X. Wang, "Glycemic variability: Importance, relationship with physical activity, and the influence of exercise," *Sports Medicine and Health Science*, vol. 3, no. 4, pp. 183–193, 2021.

[14] V. W. Bolie, "Coefficients of normal blood glucose regulation," *Journal of applied physiology*, vol. 16, no. 5, pp. 783–788, 1961.

[15] R. N. Bergman, Y. Z. Ider, C. R. Bowden, and C. Cobelli, "Quantitative estimation of insulin sensitivity.," *American Journal of Physiology-Endocrinology And Metabolism*, vol. 236, no. 6, p. E667, 1979.

[16] P. T. Saunders, J. H. Koeslag, and J. A. Wessels, "Integral rein control in physiology," *Journal of Theoretical Biology*, vol. 194, no. 2, pp. 163–173, 1998.

[17] S. Masroor, M. G. van Dongen, R. Alvarez-Jimenez, K. Burggraaf, L. A. Peletier, and M. A. Peletier, "Mathematical modeling of the glucagon challenge test," *Journal of pharmacokinetics and pharmacodynamics*, vol. 46, no. 6, pp. 553–564, 2019.

[18] P. Goel, D. Parkhi, A. Barua, M. Shah, and S. Ghaskadbi, "A minimal model approach for analyzing continuous glucose monitoring in type 2 diabetes," *Frontiers in physiology*, vol. 9, p. 673, 2018.

[19] K. Bartlette, A.-M. Carreau, D. Xie, Y. Garcia-Reyes, H. Rahat, L. Pyle, K. J. Nadeau, M. Cree-Green, and C. D. Behn, "Oral minimal model-based estimates of insulin sensitivity in obese youth depend on oral glucose tolerance test protocol duration," *Metabolism open*, vol. 9, p. 100078, 2021.

[20] L. v. Veen, J. Morra, A. Palanica, and Y. Fossat, "Homeostasis as a proportional–integral control system," *NPJ digital medicine*, vol. 3, no. 1, pp. 1–7, 2020.

[21] E. Ng, J. M. Kaufman, L. van Veen, and Y. Fossat, "A parsimonious model of blood glucose homeostasis," *arXiv preprint arXiv:2111.07181*, 2021.

[22] H. Hall, D. Perelman, A. Breschi, P. Limcaoco, R. Kellogg, T. McLaughlin, and M. Snyder, "Glucotypes reveal new patterns of glucose dysregulation," *PLoS biology*, vol. 16, no. 7, p. e2005143, 2018.

[23] "Biofeedback of glucose in non-diabetic participants." Identifier: NCT04077203, 2020. ClinicalTrials.gov.

[24] "A triple cohort, prospective observational study to analyze type 2 diabetes." Identifier: NCT04529239, 2020. ClinicalTrials.gov.

[25] "A quadruple cohort, prospective observational study to analyze type 2 diabetes glucose biomarkers and physiological variables with continuous glucose monitoring system." Identifier: CTRI/2021/08/035957, 2021. CTRI.nic.in.

[26] I. Rix, C. Nexøe-Larsen, N. C. Bergmann, A. Lund, and F. K. Knop, "Glucagon physiology," 2015.

[27] R. S. Sherwin and L. Sacca, "Effect of epinephrine on glucose metabolism in humans: contribution of the liver," *American Journal of Physiology-Endocrinology And Metabolism*, vol. 247, no. 2, pp. E157–E165, 1984.

[28] A. A. Gupte, H. J. Pownall, and D. J. Hamilton, "Estrogen: an emerging regulator of insulin action and mitochondrial function," *Journal of diabetes research*, vol. 2015, 2015.

[29] D. G. Maki, "Hba1c has low accuracy for prediabetes; lifestyle programs and metformin reduce progression to t2dm," *Annals of Internal Medicine*, vol. 166, no. 8, pp. JC41–JC41, 2017.

[30] C. S. Göbl, L. Bozkurt, M. Mittlböck, M. Leutner, R. Yarragudi, A. Tura, G. Pacini, and A. Kautzky-Willer, "To explain the variation of ogtt dynamics by biological mechanisms: a novel approach based on principal components analysis in women with history of gdm," *American Journal of Physiology-Regulatory, Integrative and Comparative Physiology*, vol. 309, no. 1, pp. R13–R21, 2015.

[31] P. A. Kaufman, K. J. Bloom, H. Burris, J. R. Gralow, M. Mayer, M. Pegram, H. S. Rugo, S. M. Swain, D. A. Yardley, M. Chau, *et al.*, "Assessing the discordance rate between local and central her2 testing in women with locally determined her2-negative breast cancer," *Cancer*, vol. 120, no. 17, pp. 2657–2664, 2014.

[32] A. G. Tabák, C. Herder, W. Rathmann, E. J. Brunner, and M. Kivimäki, "Prediabetes: a high-risk state for developing diabetes," *Lancet*, vol. 379, no. 9833, p. 2279, 2012.

[33] L. D. Maxim, R. Niebo, and M. J. Utell, "Screening tests: a review with examples," *Inhalation toxicology*, vol. 26, no. 13, pp. 811–828, 2014.

[34] M. Petticrew, A. Sowden, and D. Lister-Sharp, "False-negative results in screening programs: Medical, psychological, and other implications," *International journal of technology assessment in health care*, vol. 17, no. 2, pp. 164–170, 2001.

[35] F. J. Dallo and S. C. Weller, "Effectiveness of diabetes mellitus screening recommendations," *Proceedings of the National Academy of Sciences*, vol. 100, no. 18, pp. 10574–10579, 2003.

[36] G. Kaur, P. Lakshmi, A. Rastogi, A. Bhansali, S. Jain, Y. Teerawattananon, H. Bano, and S. Prinja, "Diagnostic accuracy of tests for type 2 diabetes and prediabetes: A systematic review and meta-analysis," *PloS one*, vol. 15, no. 11, p. e0242415, 2020.

[37] E. Barry, S. Roberts, J. Oke, S. Vijayaraghavan, R. Normansell, and T. Greenhalgh, "Efficacy and effectiveness of screen and treat policies in prevention of type 2 diabetes: systematic review and meta-analysis of screening tests and interventions," *bmj*, vol. 356, 2017.

[38] D. S. Mshelia, S. Adamu, and R. M. Gali, "Oral glucose tolerance test (ogtt): Undeniably the first choice investigation of dysglycaemia, reproducibility can be improved," in *Type 2 Diabetes-From Pathophysiology to Cyber Systems*, IntechOpen, 2021.